NASA CR- 152477

SSC

FINAL REPORT

# EVALUATION OF NASA SPEECH ENCODER

CONTRACT NAS5-23460

(NASA-CR-152477) EVALUATION OF NASA SPEECH ENCODER Final Report (Southeastern Scientific Co., Inc.) 79 p HC A05/MF A01 CSCL 14B

N77-21401

Unclas

G3/35 24440

December 15, 1976



Prepared for

NATIONAL AERONAUTICS AND SPACE ADMINISTRATION

Goddard Space Flight Center

Greenbelt, Maryland 20771

Southeastern Scientific Company, Inc.

# FINAL REPORT

## EVALUATION OF NASA SPEECH ENCODER

CONTRACT NAS5-23460

NATIONAL AERONAUTICS AND SPACE ADMINISTRATION
Goddard Space Flight Center
Greenbelt, Maryland 20771

Prepared by

Southeastern Scientific Co., Inc.
P. O. Box 8721
University Station
Knoxville, TN 37916

December 15, 1976

TABLE OF CONTENTS

# COMPUTER SIMULATION AND ANALYSIS OF A VOICE DECODING QUANTIZER

## 1. INTRODUCTION

Over the past twenty-five years man's only direct communication with digital computing systems has been through switches and typewriter keyboards. A significant fraction of the cost incurred in operating modern computing facilities is related to software development and man-machine interaction. The years ahead show promise of direct verbal communication with computers, a capability which would not only improve efficiency of operation, but would also pave the way for truly general utilization of computing systems by a large segment of potential users.

Interaction with computers, although an important area, is not the only application of automatic speech processing. A system capable of breaking down speech into its basic building blocks (i.e., phonemes) would find application in almost every field of voice communication because of the considerable reductions in bandwidth that would be possible with this approach. A system of this nature would also have other social benefits such as helping the deaf to understand the spoken word by developing machines that preprocess speech and output its phoneme content on a portable display. Since deaf

individuals usually have a speaking handicap because they cannot hear themselves, a simpler system could also be developed to teach a deaf person correct pronunciation by using biofeedback procedures.

The techniques which NASA has pioneered for the development of space flight instrumentation are ideally suited for conversion to the task of speech decoding. Donald Lokerson of the NASA-Goddard Space Flight Center recognized this similarity, and he designed a quantizer to decode speech phonemes and sounds using many of the same techniques which he developed for spaceflight electronic equipment (1). This quantizer is a hardware device subject to the variability of electronic components. The purpose of the project reported in the following sections was to simulate the action of the quantizer in a digital computer where such parameters as gain, quantizer levels, thresholds, and filters could be controlled easily and precisely. At this stage of investigation into Lokerson's idea, simulation is a valuable tool because changes in the system can be made at a fraction of the cost required to modify a hardware prototype. After the quantizer was simulated in a computer, its operation was tested with synthesized as well as real speech signals. All results were evaluated by a specialist on speech phonetics.

# 2. COMPUTER SIMULATION OF VOICE-DECODING SYSTEM

## 2.1 OVERVIEW OF THE SIMULATION APPROACH

The entire voice-decoding system was simulated in a minicomputer. Figure 1 shows a block diagram of the simulation. Signals were derived from two sources: (1) a phonetician interacting with the computer via a microphone, and (2) computer generated waveforms. The first source was used for on-line evaluation of the system. The second source was used for studying system performance under controlled conditions.

After a signal is digitized, it is processed by three digital filters to produce the three speech formants. The outputs of these filters are then fed into a simulation of Lokerson's decoding quantizer to obtain three trains of pulses. The number of pulses is monitored by software pulse counters. After a given segment of a speech signal has been processed, or after the counter for the second formant output reaches a specified count, the formant ratios $F_1/F_2$ and $F_3/F_2$ are computed. These ratios are then used to identify the nature of the input sound. They can be displayed on a two-dimensional plot with $F_1/F_2$ and $F_3/F_2$ axes, or tabulated on a printer for later reference.

## 2.2 OPERATION OF THE QUANTIZER

The objective of the quantizer is to produce trains of pulses which are proportional to the frequency and amplitude

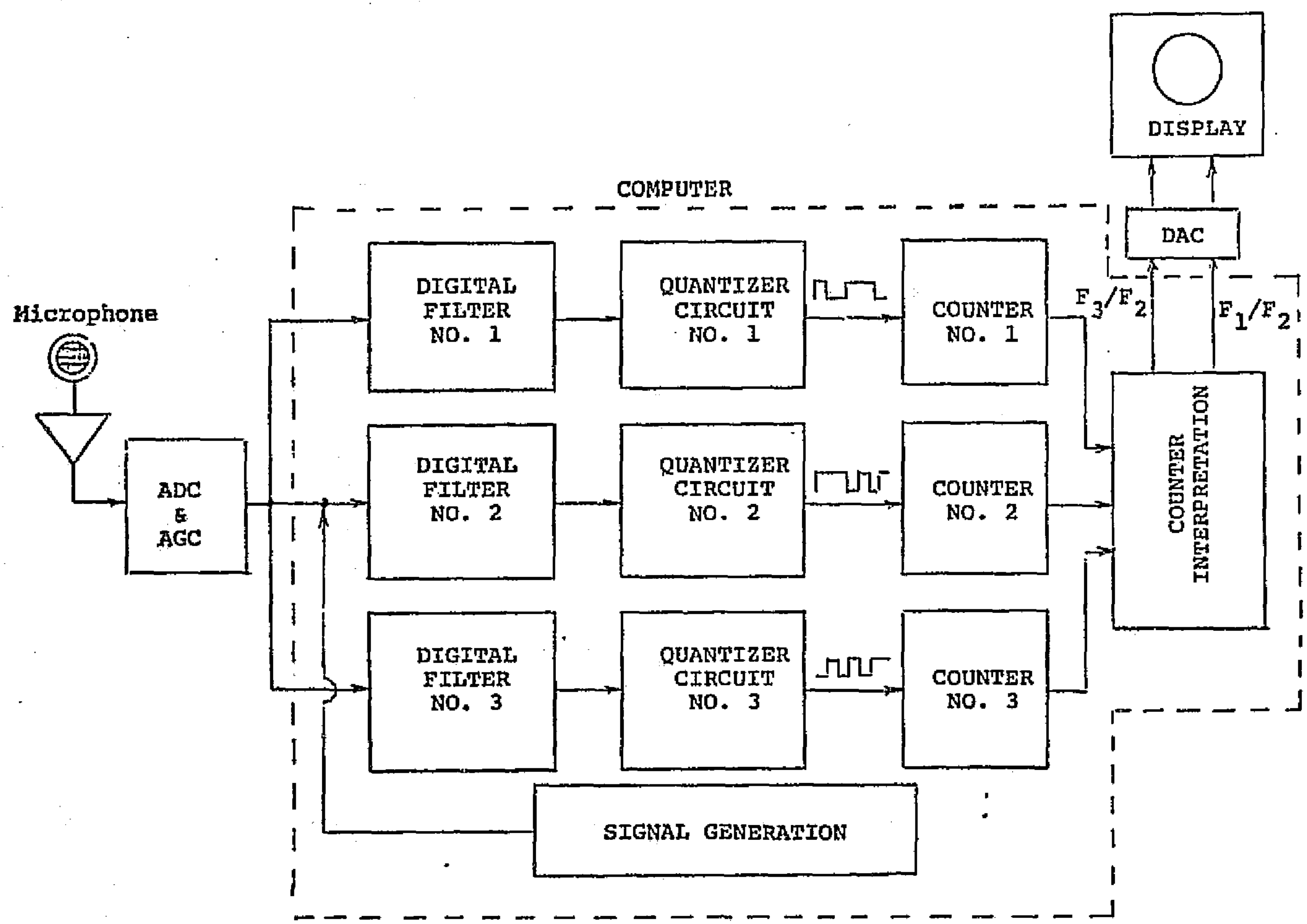


Figure 1. Block diagram of computer simulation

of the three filtered input signals. The operation of the quantizer can be illustrated by means of the simple waveforms shown in Figure 2. Assume the $g_1(t)$, $g_2(t)$ and $g_3(t)$ are the inputs to quantizers 1, 2, and 3, respectively. In this case $g_1(t)$ and $g_3(t)$ are equal. The quantizer requires three parameters: the number of levels, amplitude of the maximum and minimum levels, and specification of a stopping point in time for computation of the formant ratios $F_1/F_2$ and $F_3/F_2$. In the example shown in Figure 2, there are two levels in the positive region and (by symmetry) two levels in the negative region. For the purpose of illustration it is assumed that the maximum quantizer levels are set equal to the maximum signal amplitude. The pulse trains are generated in the following manner: In the positive region, a pulse is initiated whenever a signal enters an odd band (i.e., the bands between levels 0-1, 2-3, 5-6, etc.) and terminated when it enters an even band. The opposite is true for the negative region. Consider, for example, the pulses generated by $g_2(t)$ in Figure 2. The signal starts in band 1, defined by levels 0 and 1. Since this is an odd band, and the signal is in the positive region, a pulse is is initiated and continued until $g_2(t)$ enters band 2. As shown in the pulse diagram, the pulse drops for as long as $g_2(t)$ is in this band. When $g_2(t)$ goes back into band 1, a new pulse is started. This pulse is terminated when the signal enters band 1 in the negative region, and restarted when

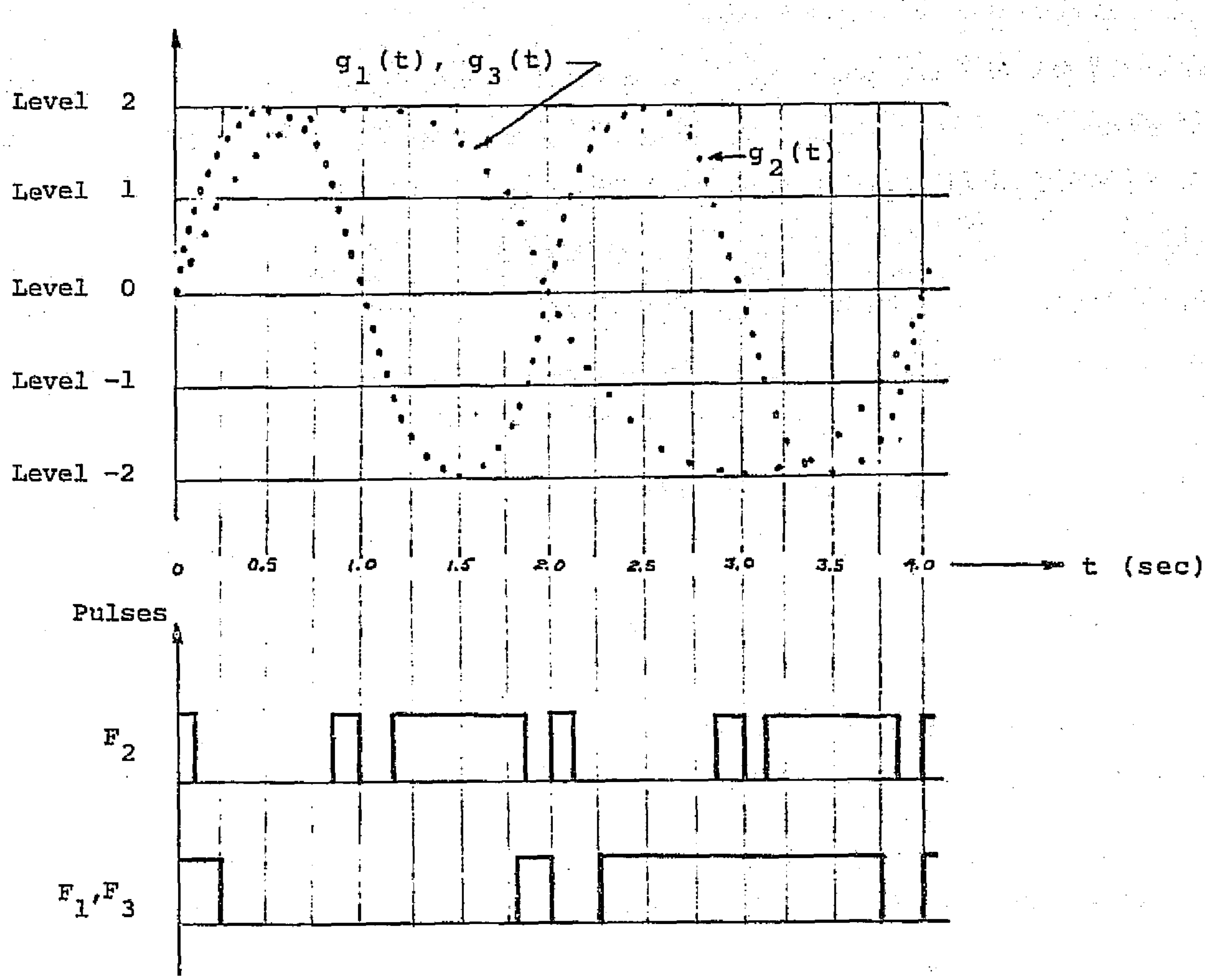


Figure 2. Examp… of quantizer operation

it enters band 2 in that region. Application of this procedure yielded the two train pulses shown in the figure. If, for example, the quantizer were stopped at $t = 4$ sec., we would have the ratios $F_1/F_2 = F_3/F_2 = 0.5$ since there would be twice as many pulses for $F_2$ than for $F_1$ or $F_3$.

## 2.3 RELATIONSHIP BETWEEN THE NUMBER OF QUANTIZER LEVELS AND THE REQUIRED SAMPLING RATE

As indicated in the previous section, the number of pulses output by the quantizer is determined by the number of transitions between quantizer bands in a given time period. When a signal is digitized, therefore, it is important that there be at least one sample per band to assure that transitions between bands are properly accounted for. In the following discussion we consider the required sampling rate as a function of the number of levels used in the quantizer.

Let Q be the number of levels used in the positive region of the quantizer† and consider a function $g(t) = A\sin 2\pi ft$, where f is the signal frequency in Hz. If this function is sampled at time increments $\Delta t = t_i - t_{i-1}$ we see that the change of g(t) between samples is

$$\begin{aligned} \Delta g &= g(t_i) - g(t_{i-1}) \\ &= A\sin 2\pi ft_i - A\sin 2\pi ft_{i-1} \end{aligned} \tag{1}$$

†By symmetry we consider the same number of levels in the negative region so that the total number of levels is 2Q.

Since the fastest rate of change of a sine function is at the origin, it is of interest to examine the behavior of $\Delta g$ in the time interval between the origin and the first sample. In this case $t_{i-1} = 0$ and $\Delta t = t_i$. Thus

$$\Delta g = A\sin 2\pi f \Delta t \tag{2}$$

If the levels are spaced uniformly and the maximum level is set at amplitude A, we have that their spacing is A/Q. In order to get at least one sample between any two levels, we then require that

$$\Delta g < \frac{A}{Q} \tag{3}$$

or

$$\frac{1}{Q} > \sin 2\pi f \Delta t \tag{4}$$

Solving for $\Delta t$ we have that the separation between samples for a sine wave has to be, at least,

$$\Delta t < \frac{1}{2\pi f} \sin^{-1} \left(\frac{1}{Q}\right) \tag{5}$$

where it is assumed that $\sin^{-1}$ (1/Q) is given in radians. If it is given in degrees, we have the simple conversion

$$\Delta t < \frac{1}{2\pi f} \sin^{-1} \left(\frac{1}{Q}\right) \left(\frac{\pi}{180}\right) \tag{6}$$

or

$$\Delta t < \frac{1}{360f} \sin^{-1} \left(\frac{1}{Q}\right) \tag{7}$$

The required sampling rate in samples/sec (or Hz) is simply $1/\Delta t$. Several values of Q with their required sampling rates are shown in Table 1 for f = 3500 Hz. It is noted that if Q = 32 a sampling rate in excess of 700 KHz is required.

TABLE 1

| Q | $\sin^{-1}(\frac{1}{Q})$ (deg) | $\Delta t$ (μsec) | sampling rate (KHz) |
|---|---|---|---|
| 32 | 1.791 | 1.421 | 703.6 |
| 16 | 3.583 | 2.844 | 351.6 |
| 8 | 7.181 | 5.699 | 175.5 |
| 4 | 14.478 | 11.490 | 87.0 |
| 2 | 30.000 | 23.809 | 42.0 |
| 1 | 90.000 | 71.429 | 14.0 |

Although the foregoing analysis was carried out in terms of a simple sine wave, it is indicative of the large number of samples required for proper operation of the quantizer. In the following section we consider some approaches used in obtaining an approximate solution to this problem.

## 2.4 RECONSTRUCTION OF SIGNALS

From Nyquist's sampling theorem (2) we have that a signal whose maximum frequency component is $f_{max}$ can be completely reconstructed from samples whose separation is less than $1/2f_{max}$ (i.e., a sampling rate greater than $2f_{max}$). The reconstruction formula is given by

$$f(t) = \frac{WT_s}{\pi} \sum_{n=-\infty}^{\infty} f(nT_s) \frac{\sin W(t - nT_s)}{W(t - nT_s)}, \tag{8}$$

where

$T_s = 1/f_s$, ($f_s$ is the sampling frequency),

W is a number such that $2\pi f_{max} \leq W \leq 2\pi(f_s - f_{max})$

$f(nT_x)$ are the samples of f(t) spaced by $T_s$.

The simplest form for the reconstruction formula occurs for $W = \pi/T_s$, which gives

$$f(t) = \sum_{n=-\infty}^{\infty} f(nT_s) \frac{\sin(\pi t/T_s - n\pi)}{\pi t/T_s - n\pi} \tag{9}$$

where $1/T_s = f_s \geq 2f_{max}$.

It is of interest from a practical point of view to estimate the number of terms required to give f(t) to within some specified accuracy. If we define $\hat{f}(t)$ to be the value given by the reconstruction formula when truncated to a finite summation, then we require that

$$|f(t) - \hat{f}(t)| < \varepsilon, \tag{10}$$

where $\varepsilon$ is a number we can choose. Since the terms in the series are large when $n = t/T_s$, or when $t = nT_s$, it is useful to write the reconstruction formula for $\hat{f}(t)$ in the following manner:

$$\hat{f}(t) = \sum_{n=p-N}^{p+N} f(nT_s) \frac{\sin(\pi t/T_s - n\pi)}{\pi t/T_s - n\pi} \tag{11}$$

where p is the closest integer to $t/T_s$. This truncated series contains 2N + 1 terms.

As an example, let $f(t) = \sin\pi 7000\, t$ so that $f = 3500$ Hz. This may be considered to be the highest required frequency ($f_{max}$) for voice communication. Thus, $f_s$ must be greater than 7000. Choose $f_s = 10^5/9$, or $T_s = 9 \times 10^{-5}$ as determined by practical considerations. Calculate the required number of terms (2N+1) for, (a) $\varepsilon = 1/16$, and (b) $\varepsilon = 1/32$. The reconstruction formula is

$$\hat{f}(t) = \sum_{n=p-N}^{p+N} \sin(0.063n\pi) \frac{\sin \dfrac{\pi t x 10^5}{9} - n\pi}{\dfrac{\pi t x 10^5}{9} - n\pi}$$

Results are shown in Table 2. They indicate, as expected, that the largest number of terms is required when interpolating midway between samples. Thus, values of f(t) lying between sample values can be found to any desired accuracy by increasing N. Values so calculated are equivalent to new

TABLE 2

| $t/T_s$ | $f(t)$ | $\varepsilon = 1/16$ | | $\varepsilon = 1/32$ | |
|---|---|---|---|---|---|
| | | No. of Terms | $\hat{f}(t)$ | No. of Terms | $\hat{f}(t)$ |
| 0.00000 | 0 | 1 | 0 | 1 | 0 |
| 0.01579 | 0.03125 | 1 | 0 | 1 | 0 |
| 0.25000 | 0.47486 | 13 | 0.45035 | 23 | 0.44864 |
| 0.50000 | 0.83581 | 19 | 0.83767 | 35 | 0.83179 |
| 0.75000 | 0.99627 | 7 | 1.03222 | 21 | 0.97374 |
| 0.79365 | 1.00000 | 7 | 1.03011 | 13 | 0.99041 |
| 1.00000 | 0.91775 | 1 | 0.91775 | 1 | 0.91775 |

sample values, and thus the use of the reconstruction formula is equivalent to using a much higher sampling rate. In other words, use of Equation (11) allows a much slower sampling rate for an input speech signal. If Nyquist's sampling criterion is satisfied, we are assured that it is possible to obtain any desired number of interpolated points between the sampled values. The accuracy of the new points is determined by the number of terms used in Equation (11).

All the speech signals processed in this project were lowpass filtered at 3500 Hz prior to sampling in order to avoid aliasing. The sampling rate used was 11 KHz which is well

above the required Nyquist rate of 7 KHz. After sampling, each input signal was filtered into three formant regions, as discussed in Figure 1, and the three resulting signals were reconstructed to a rate specified from the computer keyboard.

Since, as shown in Table 1, the required effective sampling rates are quite high, an approximation was used in the quantizer which allowed utilization of much lower rates. The approximation consisted of treating successive samples as if they were joined by a straight line. In this way erroneous transitions between levels were minimized for signals whose (reconstructed) sampling rates were below those indicated in Table 1.

To illustrate the behavior of this approach, three sine waves of 500, 1000, and 3000 Hz were created in the computer at a sampling rate of 100 KHz. Eighty blocks of data of 128 samples each were generated for each function and fed into the quantizer with and without the straight line approximation. Q = 32 was used in both cases which, according to the figures in Table 1, should have required a sampling rate of about 700 KHz for the 3000 Hz sine wave. After processing all 80 blocks without the straight line approximation the formant ratios were $F_1/F_2 = 0.775$ and $F_3/F_2 = 1.15$. With the straight line approximation the results were $F_1/F_2 = 0.501$ and $F_3/F_2 = 2.93$. These latter results are much closer to the ideal values $F_1/F_2 = 0.500$ and $F_3/F_2 = 3.000$. The results

obtained with the straight line approximation were also close for shorter processing blocks. Figure 3 shows the results for signal segments which were 8 blocks long.

| BLOCK | F1/F2 | F3/F2 | CNT FOR F1 | CNT FOR F2 | CNT FOR F3 |
|---|---|---|---|---|---|
| 8 | 0. 504 | 2. 999 | 0. 3255E+03 | 0. 6455E+03 | 0. 1936E+04 |
| 16 | 0. 498 | 3. 005 | 0. 3200E+03 | 0. 6430E+03 | 0. 1933E+04 |
| 24 | 0. 490 | 2. 995 | 0. 3180E+03 | 0. 6485E+03 | 0. 1942E+04 |
| 32 | 0. 509 | 3. 021 | 0. 3260E+03 | 0. 6405E+03 | 0. 1935E+04 |
| 40 | 0. 502 | 2. 988 | 0. 3265E+03 | 0. 6500E+03 | 0. 1942E+04 |
| 48 | 0. 504 | 3. 024 | 0. 3220E+03 | 0. 6395E+03 | 0. 1934E+04 |
| 56 | 0. 487 | 2. 975 | 0. 3170E+03 | 0. 6510E+03 | 0. 1937E+04 |
| 64 | 0. 507 | 3. 016 | 0. 3270E+03 | 0. 6445E+03 | 0. 1944E+04 |
| 72 | 0. 500 | 2. 937 | 0. 3285E+03 | 0. 6575E+03 | 0. 1931E+04 |
| 80 | 0. 510 | 3. 009 | 0. 3290E+03 | 0. 6455E+03 | 0. 1943E+04 |

Figure 3. Behavior of the quantizer with straight line approximation

## 3. DIGITAL FILTERING

The concept of digital filtering refers to the process of operating on a given digital signal to produce another digital signal. Figure 4 illustrates this process. The input signal is a sequence of numbers, $\{f_m\} = \{f_0, f_1, f_2, f_3, \ldots\}$, generally acquired from an analog-to-digital converter (ADC) or a direct digital input source. This sequence is transformed by the digital filter, a term referring to a computational algorithm performed on the input sequence, to produce an output sequence, $\{g_m\}$. The computational process can correspond to the highpass filtering, lowpass filtering, bandpass filtering, or other desired transformation.

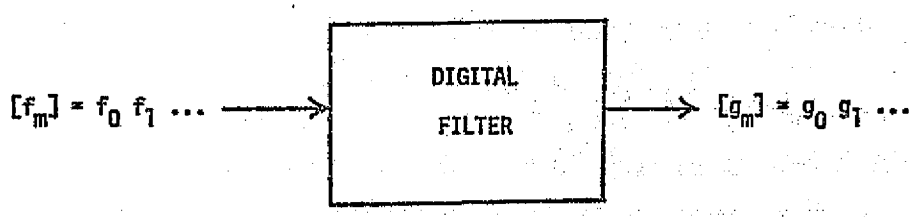


Figure 4. Process of digital filtering.

Digital transformations are most easily represented by linear difference equations. The digital process of Figure 4 is described by the general recursive equation

$$g_m = \sum_{k=0}^{K} b_k f_{m-k} - \sum_{k=1}^{K} a_k g_{m-k} \qquad (12)$$

in which the coefficient $a_k$ and $b_k$ are the characteristic coefficents of the digtal filter. Observe that $g_m$, the present output of the filter, is computed from the present and past values of the input ($f_m$, $f_{m-1}$, $f_{m-2}$, ... $f_{m-k}$) and the past values of the output ($g_{m-1}$, $g_{m-2}$, ..., $g_{m-k}$). For an input sequence which is generated periodically with period T, $g_m$ represents the filter output at $t = mT$ (i.e. $g(mT)$).

In this research, the continuous processes of speech and formant filtering were simulated by digital filtering techniques. Figure 5 describes the simulation of the continuous processes. The speech input is periodically sampled, digitized, and output to the formant filters as a sequence of numbers, $\{f_m\}$. Each of the formant filters was simulated by a digital filter and programmed on a PDP 11/40 digital computer. The computer transformed the speech sequence $\{f_m\}$ by the recursive equation of each formant filter to generate the output sequences $\{g_{1m}\}$, $\{g_{2m}\}$, and $\{g_{3m}\}$ to the quantizer.

Several advantages are offered by this simulation approach. First, a greater flexibility is achieved since the filter characteristics can be altered by simply varying the proper arithmetic coefficients. An arbritarily high precision is obtained since results are limited only by the number of bits

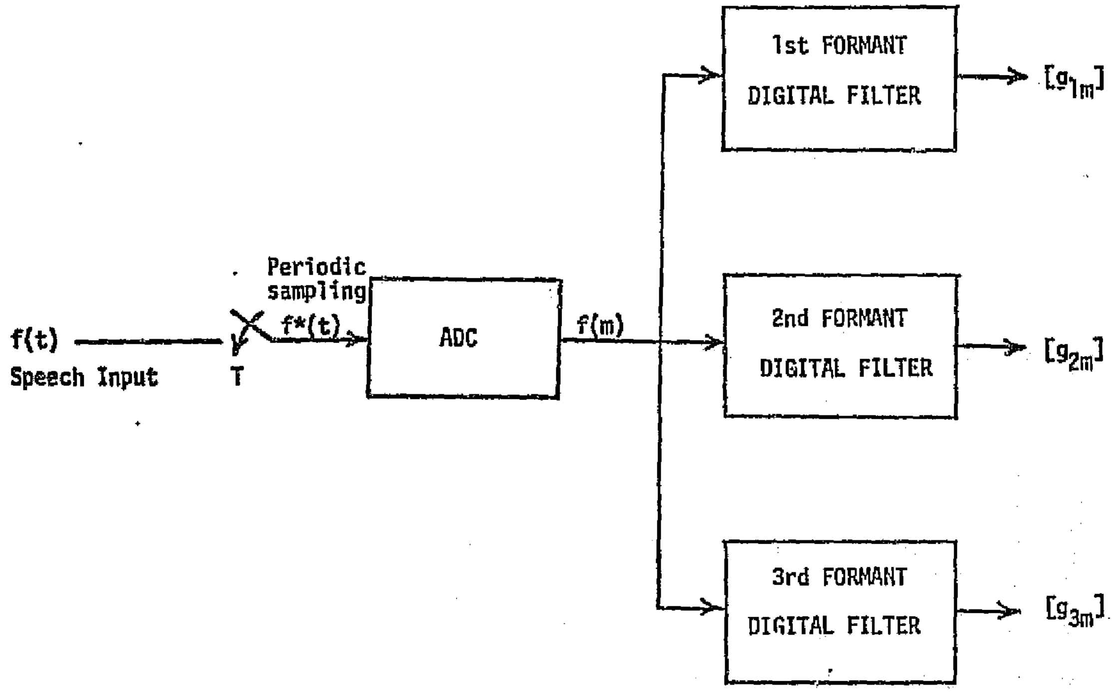


Figure 5. Digital simulation of speech and formant filtering processes. [$g_{1m}$], [$g_{2m}$], and [$g_{3m}$] are the output sequences from the formant filters and represent the inputs to the quantizer.

used to represent the filter coefficients and by the resolution of the ADC in quantizing the input. Finally, the digital filter simulation does not have the performance limitations of physical components.

A Butterworth bandpass filter was used to approximate the characteristics of the formant filters since the speech and formant filtering processes are bandpass limited. The power gain for the analog filter has the following general form:

$$|H(jw)|^2 = \frac{1}{1 + \left[\frac{w^2 - w_1 w_2}{w w_c}\right]^{2N}} \tag{13}$$

N is the order of the filter and $\frac{N}{2}$ represents the number of filter sections. The roll-off characteristics for the power gain of the filter are given as 6N db/octave. $w_1$ and $w_2$ are the half-power points of the gain and $w_c = w_2 - w_1$ is the filter bandwidth.

A digital filter is obtained from the analog filter by using the bilinear transformation to effectively transform the analog poles and zeros into digital poles and zeros. The power gain of the digital bandpass filter has the form

$$|H(jw)|^2 = \frac{1}{1 + \left[\dfrac{\tan^2 \frac{wT}{2} - w_1' w_2'}{w_c' \tan \frac{wT}{2}}\right]^{2N}} \tag{14}$$

where
$$w_1' = \tan \frac{w_1 T}{2} \tag{15}$$

$$w_2' = \tan \frac{w_2 T}{2} \tag{16}$$

and
$$w_c' = w_2' - w_1' \tag{17}$$

T represents the period of the sampling frequency and corresponds to the period at which the input speech is sampled.

The linear difference equation which describes the $k^{th}$ section $k = 1, 2, \ldots, \frac{N}{2}$ of the digital filter is presented below.

$$\begin{aligned} g(mT) = {} & A(k)[f(mT) - 2f(mT-2T) + f(mT-4T)] - B(k)g(mT-T) - C(k)g(mT-2T) \\ & - D(k)g(mT-3T) - E(k)g(mT-4T) \end{aligned} \tag{18}$$

or,

$$\begin{aligned} g_m = {} & A(k)[f_m - 2\, f_{m-2} + f_{m-4}] + B(k)g_{m-1} - C(k)g_{m-2} - D(k)g_{m-3} \\ & - E(k)g_{m-4} \end{aligned} \tag{19}$$

A Fortran computer program for the design of digital bandpass filters is shown in Figure 6. The inputs to the subroutine are the half power points $f_1$ and $f_2$ in Hz, the sampling interval T in seconds, the number NS of filter sections, and the number NF of the particular formant filter. The output generated by the program is NS sets of filter coefficients, A(k) through E(k) for k = 1, 2, ..., N/2.

After each formant filter was designed and simulated by the above approach, the sampled speech input, $f_m$ , was operated on in parallel by the formant filters to generate the quantizer inputs, $g_{1m}$ , $g_{2m}$ , and $g_{3m}$ . This approach provided a systematic method for determining and evaluating the effects of the filter characteristics on the quantizer output.

```
      SUBROUTINE BPDES(F1,F2,T,NS,NF)
      COMMON A(10,10),B(10,10),C(10,10),D(10,10),E(10,10),GRAF(10,2,20)
      DIMENSION F1(10),F2(10)
      PI=3.1415926536
      W1=SIN(F1(NF)*PI*T)/COS(F1(NF)*PI*T)
      W2=SIN(F2(NF)*PI*T)/COS(F2(NF)*PI*T)
      WC=W2-W1
      Q=WC*WC+2.*W1*W2
      S=W1*W1*W2*W2
      DO 150 K=1,NS
      CS=COS(FLOAT(2*(K+NS)-1)*PI/FLOAT(4*NS))
      P=-2.*WC*CS
      R=P*W1*W2
      X=1.+P+Q+R+S
      A(NF,K)=WC*WC/X
      B(NF,K)=(-4.-2.*P+2.*R+4.*S)/X
      C(NF,K)=(6.-2.*Q+6.*S)/X
      D(NF,K)=(-4.+2.*P-2.*R+4.*S)/X
150   E(NF,K)=(1.-P+Q-R+S)/X
      DO 160 J=1,2
      DO 160 I=1,10
      K=I*(2-J)+(21-I)*(J-1)
      GRAF(NF,2,K)=.01+.98*FLOAT(I-1)/9.
      X=(1./GRAF(NF,2,K)-1.)**(1./FLOAT(4*NS))
      SQ=SQRT(WC*WC*X*X+4.*W1*W2)
160   GRAF(NF,1,K)=ABS(ATAN(.5*(WC*X+FLOAT(2*J-3)*SQ)))/(PI*T)
      RETURN
      END
```

Figure 6. BPDES: A bandpass Butterworth digital filter design subroutine.

# 4. EXPERIMENTAL RESULTS

## 4.1 SPEECH DATA

In addition to sinusoidal data generated in the computer, the speech decoder was tested with speech data generated by two trained phoneticians. The first speaker was a woman with a highly-pitched voice, and the second a man with a deep voice. Two sets of sounds were generated by each speaker. The first set consisted of sustained vowels and the second of short words containing these vowels. The vowels and corresponding words used were

| | |
|---|---|
| i | heed |
| æ | had |
| a | hod |
| ɔ | hawed |
| u | who'd |
| ɜ̂ | heard |

In the following discussion we refer to the woman as speaker 1 and the man as speaker 2. The code

X.YZ

will be used to denote the sound, speaker, and sample number, in that order. For example, sample number 1 of the sound "i" spoken by speaker number 2 will be denoted by i.21.

The data in Table 3 will be used as a basis for evaluating system performance. The main points of interest in this table are the formant frequencies for the vowels spoken by men, women, and children. In interpreting the entries in this table the reader should keep in mind that the results were obtained by averaging a number of speakers and also that the approach we have simulated is different from simply obtaining the principal frequency of each formant.

In order to obtain a measure of expected location and separation between vowels, the ratios $F_1/F_2$ and $F_3/F_2$ were computed from the data in Table 3 and plotted on the formant space shown in Figure 7. The extremes of each rectangle were established by the extreme values of the formant ratios when men, women, and children were considered. It is important to note that the formant space shown in Figure 7 is divided mainly into five disjoint regions in the $F_1/F_2$ axis, but only two principal regions in the $F_3/F_2$ axis.

## 4.2 SPEECH RECORDING, SAMPLING, AND STORAGE

All the speech sounds described in the previous section were recorded on audio tape. The tape was then played back into the computer analog-to-digital converter for digitization. All signals were lowpass filtered at 3500 Hz (to avoid aliasing) before digitization at 11 KHz. Sixty blocks of data of 256 samples each were generated from each speech sound and stored on computer magnetic tape for further processing.

Table 3. Averages of fundamental frequencies and the first three formant frequencies of vowels produced by seventy-six speakers: thirty-three men, twenty-eight women, fifteen children. [*Table from* Handbook of Speech Pathology, *edited by Lee Edward Travis.*] *Appleton-Century-Crofts, Educational Division, Meredith Corp., 1957.*

| | | i | ɪ | ɛ | æ | ɑ | ɔ | ʊ | u | ʌ | ɝ |
|---|---|---|---|---|---|---|---|---|---|---|---|
| *Fundamental Frequencies (Hz)* | *M* | *136* | *135* | *130* | *127* | *124* | *129* | *137* | *141* | *130* | *133* |
| | *W* | *235* | *232* | *223* | *210* | *212* | *216* | *232* | *231* | *221* | *218* |
| | *Ch* | *272* | *269* | *260* | *251* | *256* | *263* | *276* | *274* | *261* | *261* |
| Formant Frequencies (Hz) | | | | | | | | | | | |
| $F_1$ | M | 270 | 390 | 530 | 660 | 730 | 570 | 440 | 300 | 640 | 490 |
| | W | 310 | 430 | 610 | 860 | 850 | 590 | 470 | 370 | 760 | 500 |
| | Ch | 370 | 530 | 690 | 1010 | 1030 | 680 | 560 | 430 | 850 | 560 |
| $F_2$ | M | 2290 | 1990 | 1840 | 1720 | 1090 | 840 | 1020 | 870 | 1190 | 1350 |
| | W | 2790 | 2480 | 2330 | 2050 | 1220 | 920 | 1160 | 950 | 1400 | 1640 |
| | Ch | 3200 | 2730 | 2610 | 2320 | 1370 | 1060 | 1410 | 1170 | 1590 | 1820 |
| $F_3$ | M | 3010 | 2550 | 2480 | 2410 | 2440 | 2410 | 2240 | 2240 | 2390 | 1690 |
| | W | 3310 | 3070 | 2990 | 2850 | 2810 | 2710 | 2680 | 2670 | 2780 | 1960 |
| | Ch | 3730 | 3600 | 3570 | 3320 | 3170 | 3180 | 3310 | 3260 | 3360 | 2160 |

## 4.3 FORMANT FILTER SETTINGS

The settings for the three formant filters were chosen to span the extremes of all the formant frequencies in Table 3. The filters used were overlapping bandpass filters with settings

F1: 225-1050 Hz

F2: 800-3300 Hz

F3: 2100-3800 Hz

Experiments with nonoverlapping filters covering the same overall range were tested early in the investigation and then discarded because they yielded poor formant-ratio results.

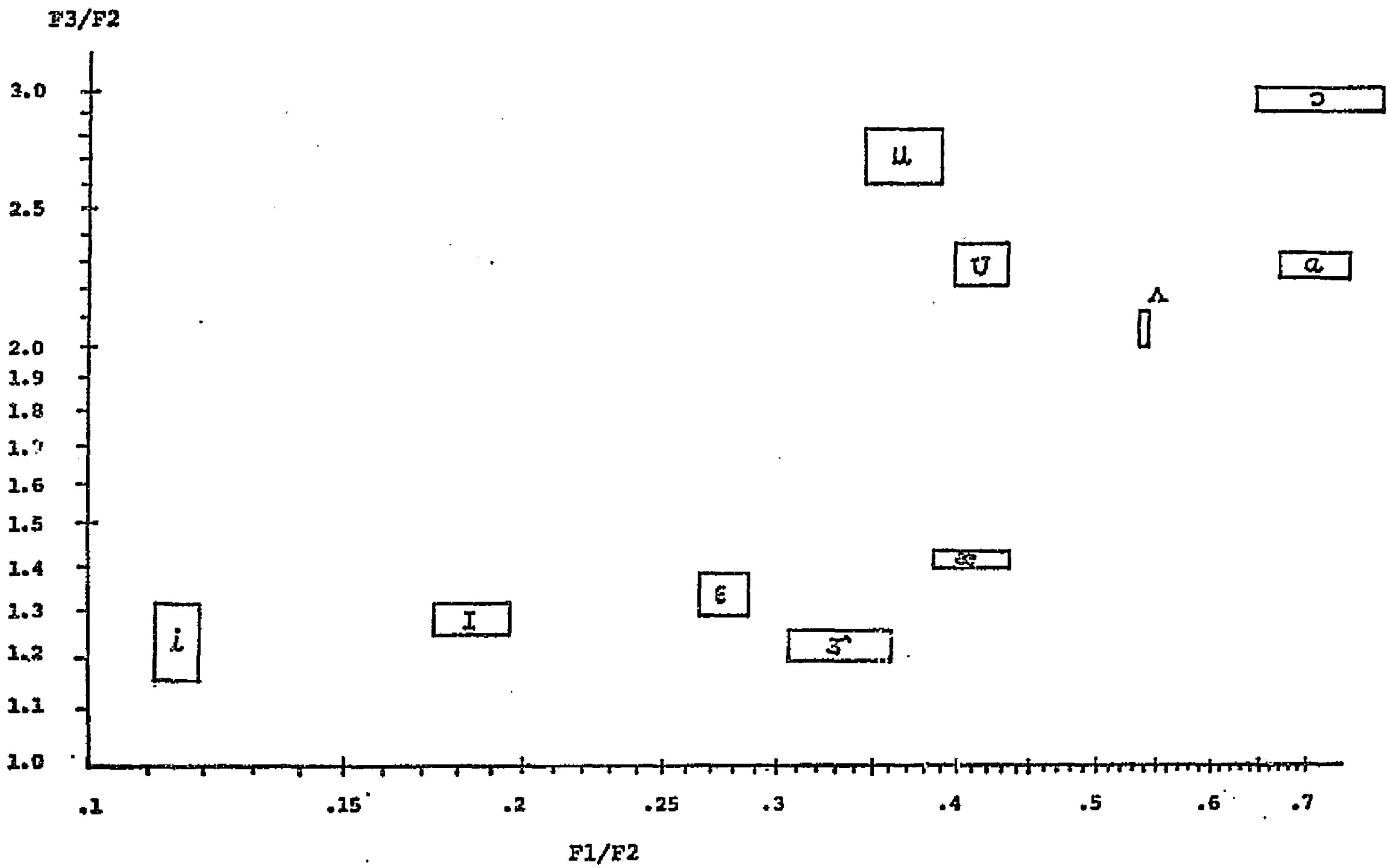


Figure 7. Formant space

## 4.4 SELECTION AND SETTING OF QUANTIZER LEVELS

Implementation of the quantizer requires a choice on the number of levels as well as the relative setting of the maximum and minimum levels. Experiments were conducted with several sinusoidal and speech signals to determine optimum settings for these parameters. Based on the results obtained with straight-line approximations in the quantizer (see Section 2.3) the outputs of the three formant filters discussed in the previous section were reconstructed to 100 KHz before they were input into the quantizer. Reconstruction was accomplished by using Equation (11) with N = 10 so that a total of twenty-one terms were used in calculating each interpolated point. We found this number of terms to be adequate in creating a smooth approximation between speech samples taken at 11 KHz.

Two approaches were investigated for setting the quantizer levels. The first was to set the maximum quantizer level for a segment of data (e.g., 10 msec) equal to the absolute peak value of the signal in the previous segment. The second approach was to set the maximum level equal to the absolute value of the average of the signal in the previous data segment. In both cases the minimum quantizer level was set equal to the negative of the maximum level.

In order to illustrate the relative effects of these settings, sound i.11 was processed with 32, 16, 8, 4, 2 and 1

equally-spaced levels on each side of the abscissa. Both approaches were used, with the peak or average values updated every 10 msec. The results are shown in Figure 8 for peak-value settings and in Figure 9 for average-value settings. The ranges spanned by the data for each level setting are enclosed by a labeled rectangle. Two significant improvements are evident in the average-value approach: first, the results in Figure 9 are much closer to the ideal region (inner box) and second, the regions spanned by the data tended to shrink about the ideal region as the number of levels was increased. In the case of Figure 8, on the other hand, a strong tendency to shift left is evident for 1 and 2 levels. Although this effect is also present in Figure 9, the shift is much smaller (note that the axis scales are logarithmic). It has been our experience that eight levels appear to yield results which are consistently very close to 32 levels.

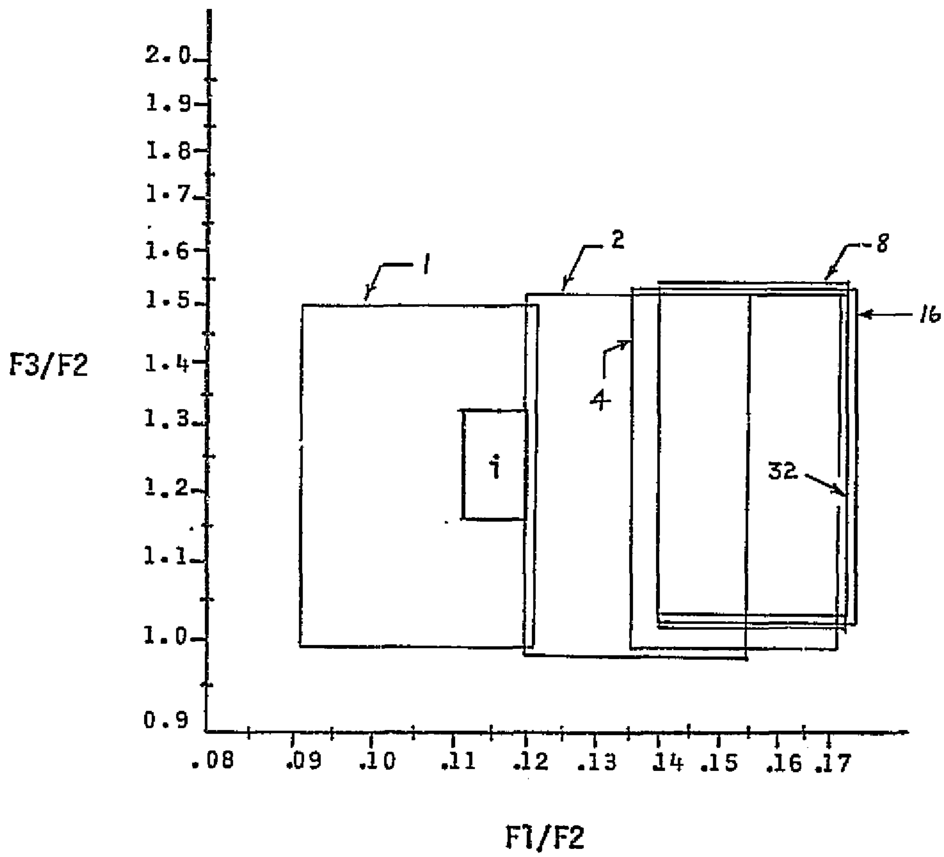
2.0
1.9
1.8
1.7
1.6
1.5
1.4
1.3
1.2
1.1
1.0
0.9
F3/F2
.08
.09
.10
.11
.12
.13
.14
.15
.16
.17
F1/F2
1
2
4
8
16
32
i

Figure 8

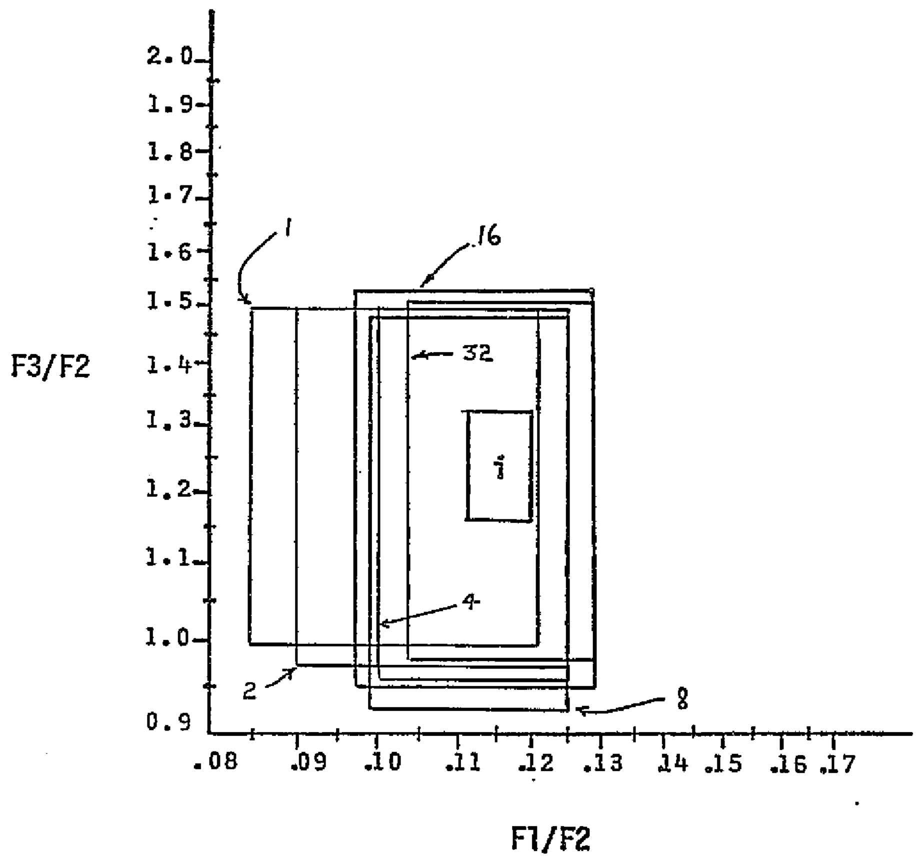
2.0
1.9
1.8
1.7
1.6
1.5
1.4
1.3
1.2
1.1
1.0
0.9
F3/F2
1
16
32
i
4
2
8
.08
.09
.10
.11
.12
.13
.14
.15
.16
.17
F1/F2

Figure 9

4.5 PROCESSING RESULTS

The vowels and words described in Section 4.1 were processed using eight positive and eight negative quantizer levels. The input speech signals were sampled at 11 KHz and filtered using the filter bandwidths given in Section 4.3. After filtering, the three formant signals were reconstructed to an effective sampling rate of 100 KHz by using Eq.(11) with N=10. The maximum and minimum quantizer levels were set using the averaging procedure described in Section 4.4. Quantization results were output every 16 blocks of reconstructed data, where each block contained 128 samples. A complete tabulation of all results is included in the Appendix.

Figure 10 is a summary of the best ratios obtained for the sustained vowels listed in Section 4.1. The entries shown in this figure are the three sets of ratios which, for each speaker, were closer to their corresponding ideal region. It is noted that for each vowel the location of F1/F2 ratio is quite close to the ideal region. The results are not as close for the F3/F2 ratios. In particular, this ratio was high for the vowel ɝ for both speakers and for the vowel æ for speaker 1. This is not unexpected since, as mentioned earlier, the formant space is divided into only two principal regions on the vertical axis.

As shown in Figure 11, similar results were obtained with the words containing the above vowels. Separation in the F1/F2 axis was as expected for all vowels. Separation in the F3/F2 axis was inadequate for ɝ (both speakers) and u and æ (speaker 1).

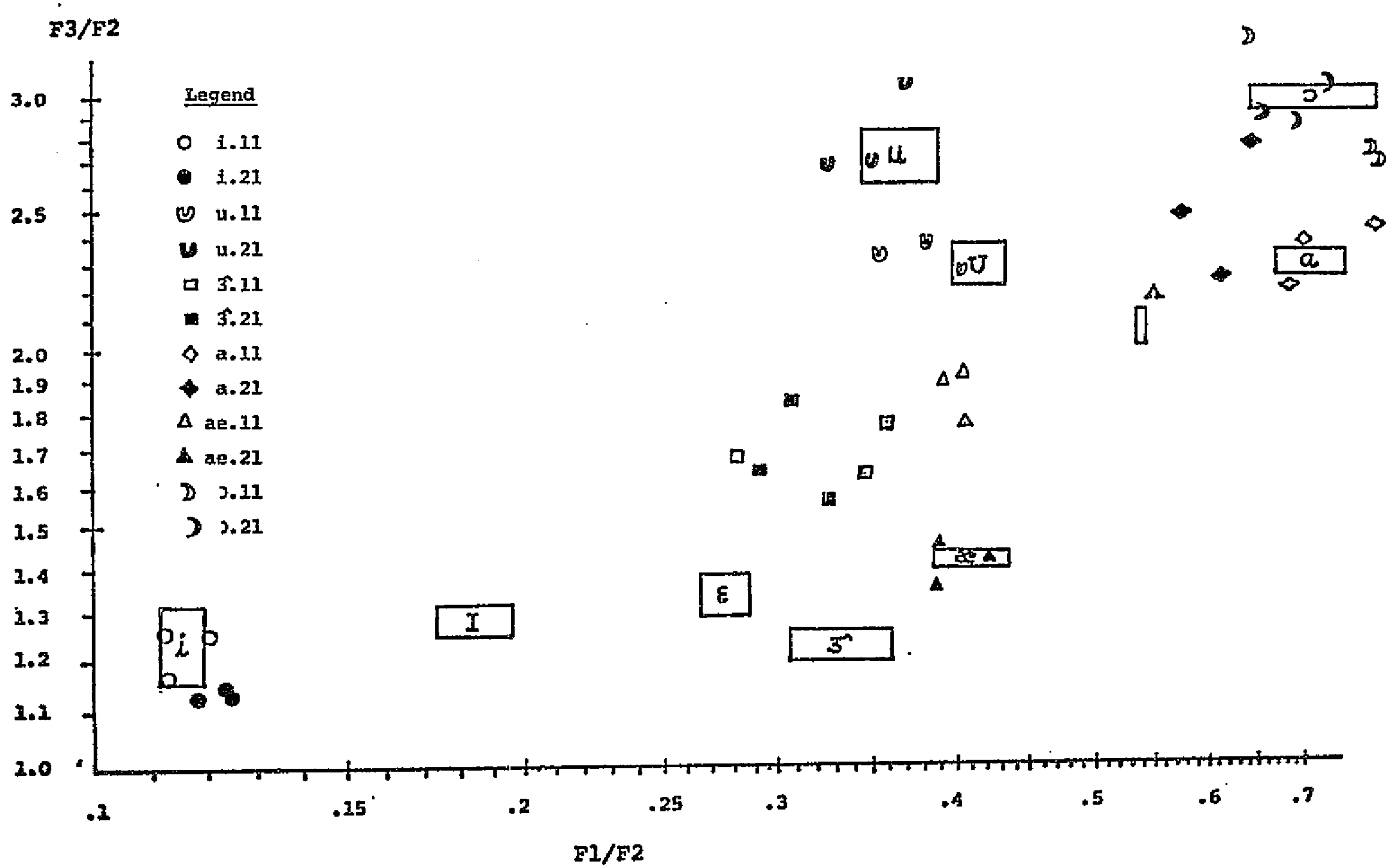
F3/F2
Legend
i.11
i.21
u.11
u.21
ɜ̂.11
ɜ̂.21
a.11
a.21
ae.11
ae.21
ɔ.11
ɔ.21
3.0
2.5
2.0
1.9
1.8
1.7
1.6
1.5
1.4
1.3
1.2
1.1
1.0
.1
.15
.2
.25
.3
.4
.5
.6
.7
F1/F2

Figure 10

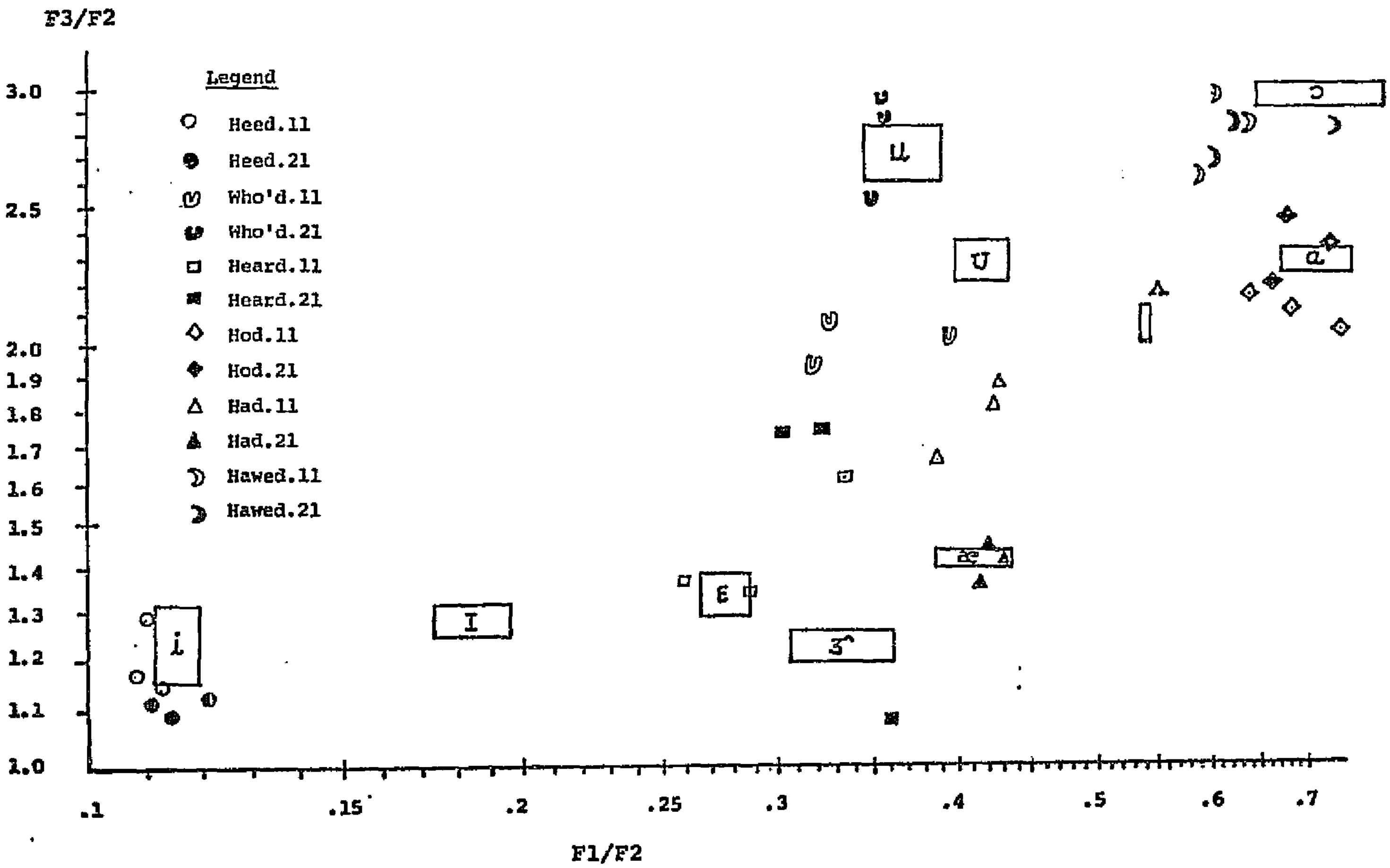
F3/F2
Legend
Heed.11
Heed.21
Who'd.11
Who'd.21
Heard.11
Heard.21
Hod.11
Hod.21
Had.11
Had.21
Hawed.11
Hawed.21
3.0
2.5
2.0
1.9
1.8
1.7
1.6
1.5
1.4
1.3
1.2
1.1
1.0
.1
.15
.2
.25
.3
.4
.5
.6
.7
F1/F2

Figure 11

Considering that the ideal formant regions in Figures 10 and 11 were obtained by averaging results over many speakers (see Section 4.1), it appears that the quantizer is performing as expected. The discrepancies on the F3/F2 axis require further attention--most likely in the filter settings and length of data blocks processed between results.

Figures 12 through 23 are plots of all the data in the Appendix. The arrow in each of these figures indicates the starting point. The principal features of these plots are the separation between vowels and the overall consistency of results between the man and woman. It is noted, however, that the formant trajectories for the man are much more clustered than those for the woman. Since the ratios were output over the same time increments, these results seem to indicate that it would be desirable to incorporate into the system some procedure for frequency normalization. One possibility is to output the ratios at the end of every pitch segment (i.e., sound burst). Implementation of this procedure would require processing the input signal prior to filtering in order to determine the individual bursts for use in stopping the pulse counters.

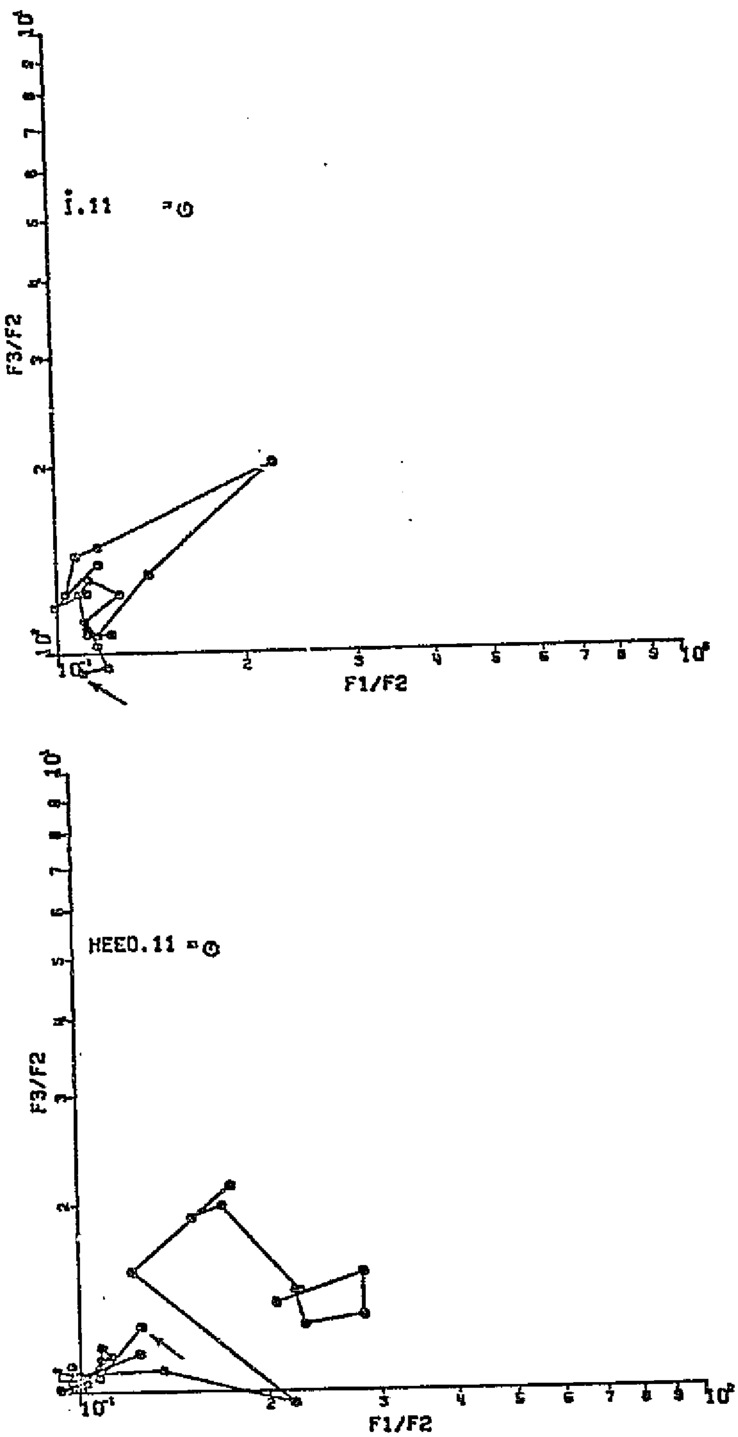


Figure 12

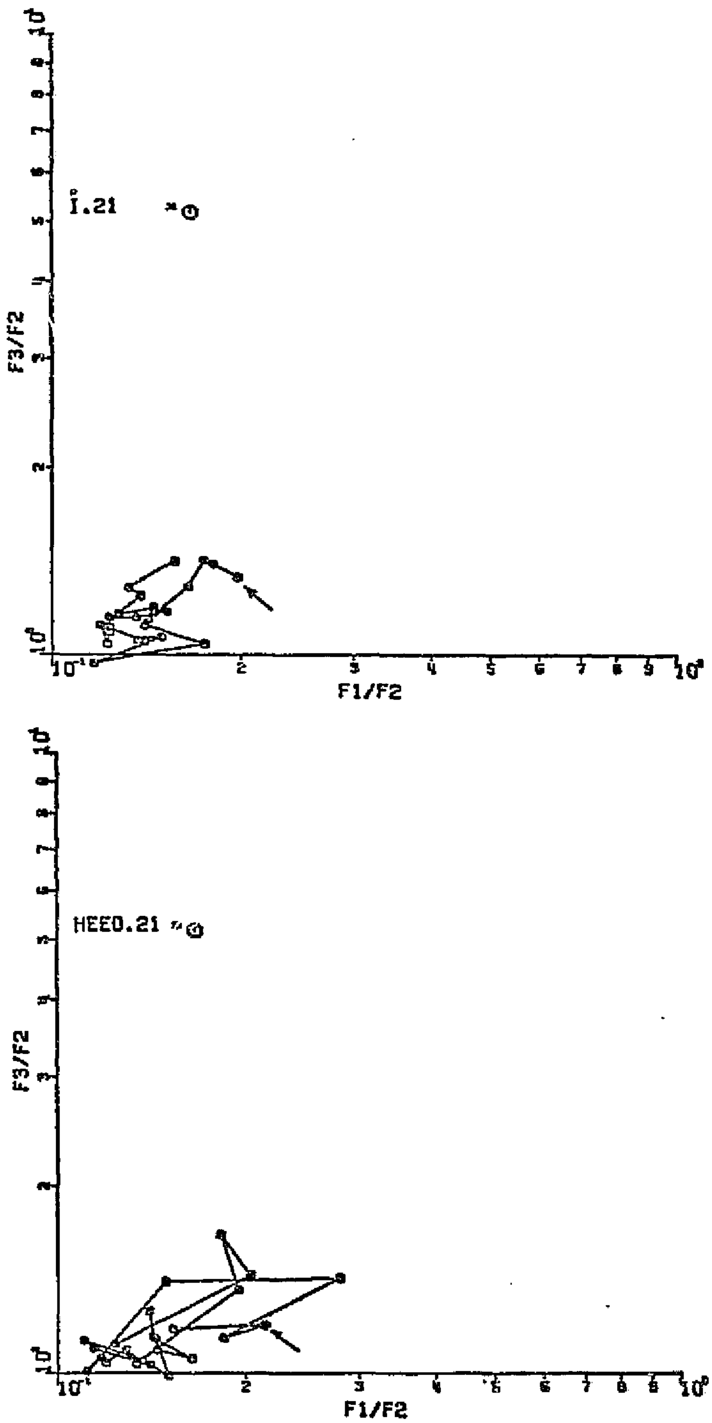


Figure 13

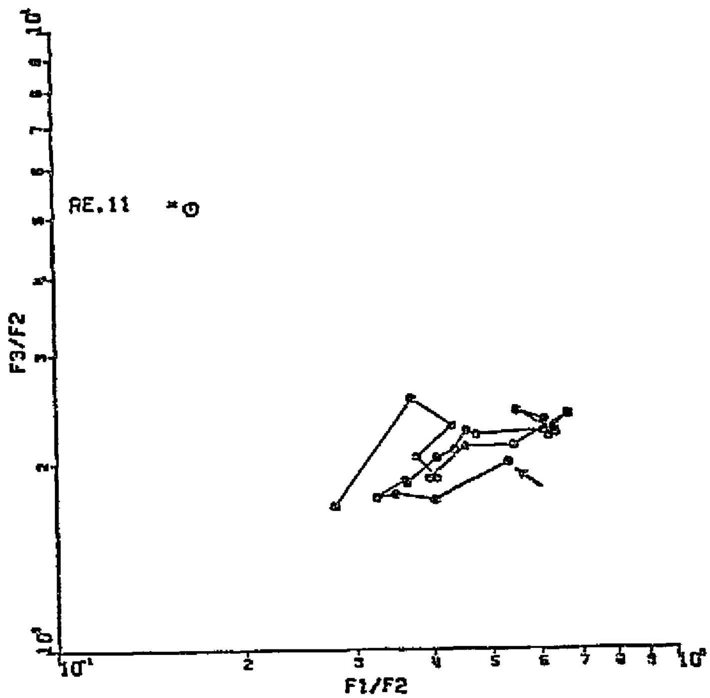


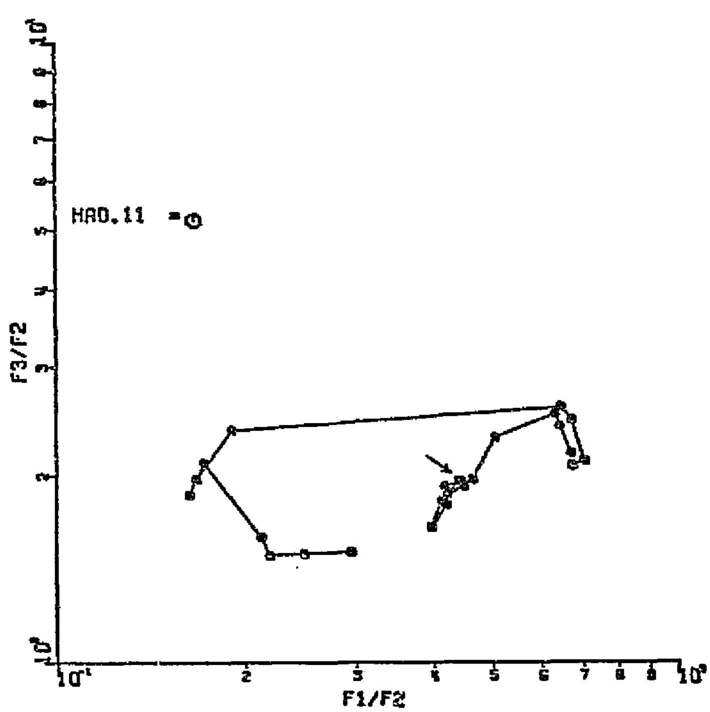


Figure 14

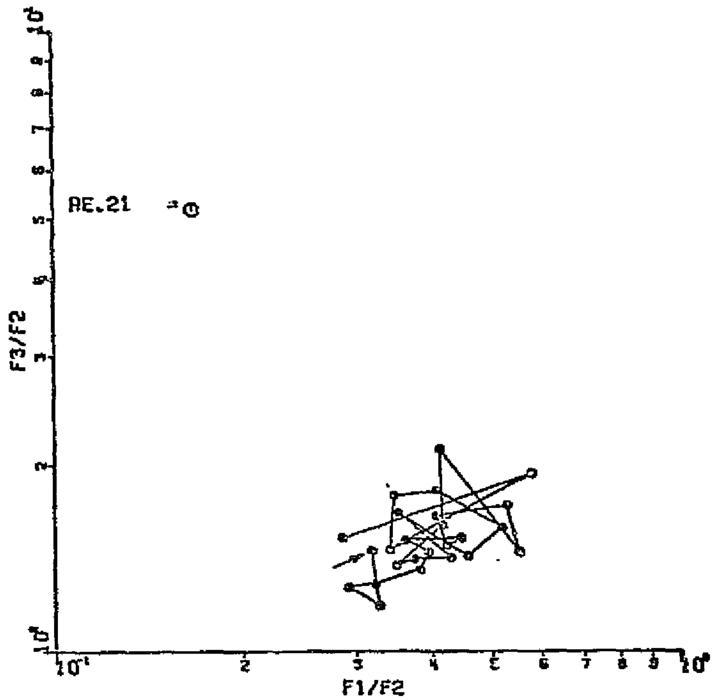


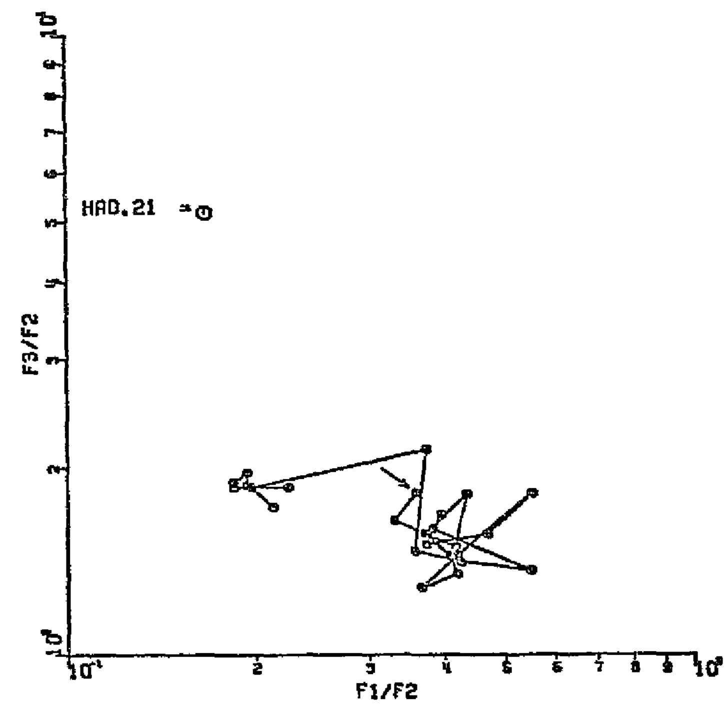


Figure 15

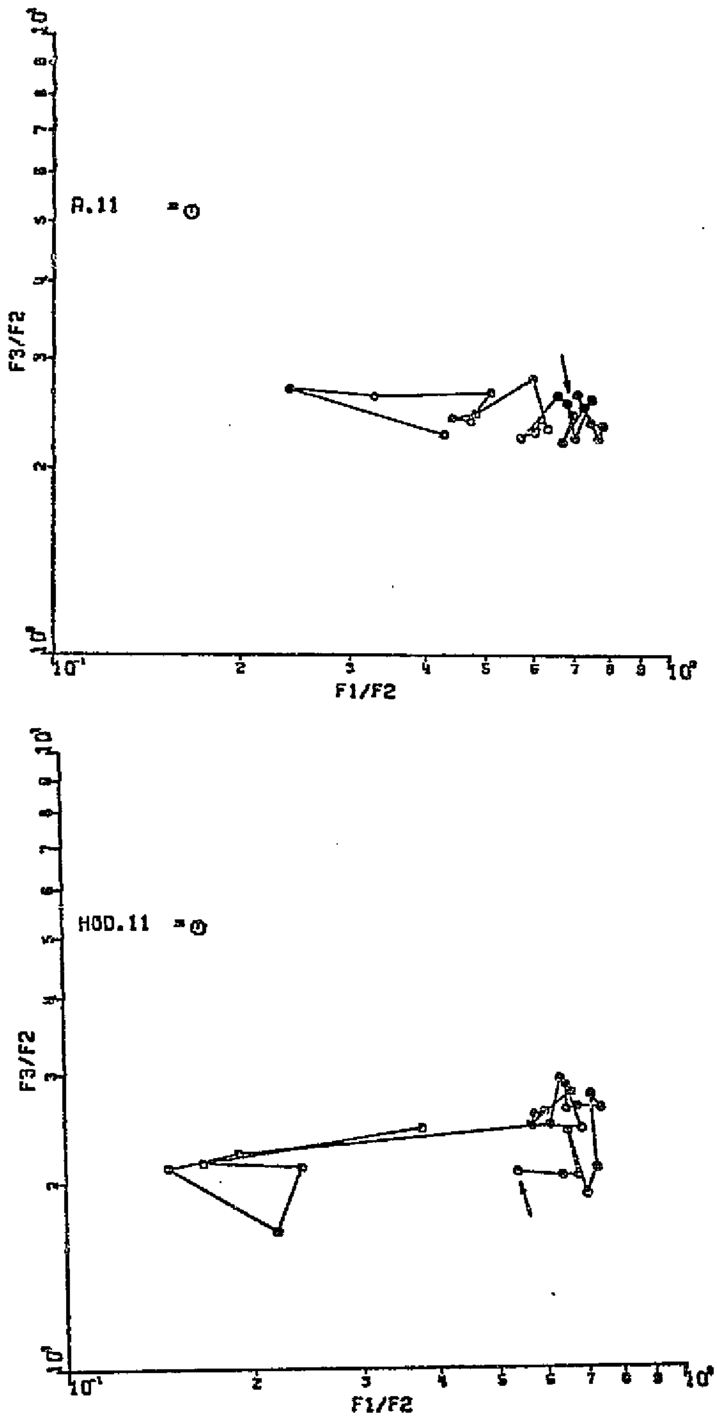


Figure 16

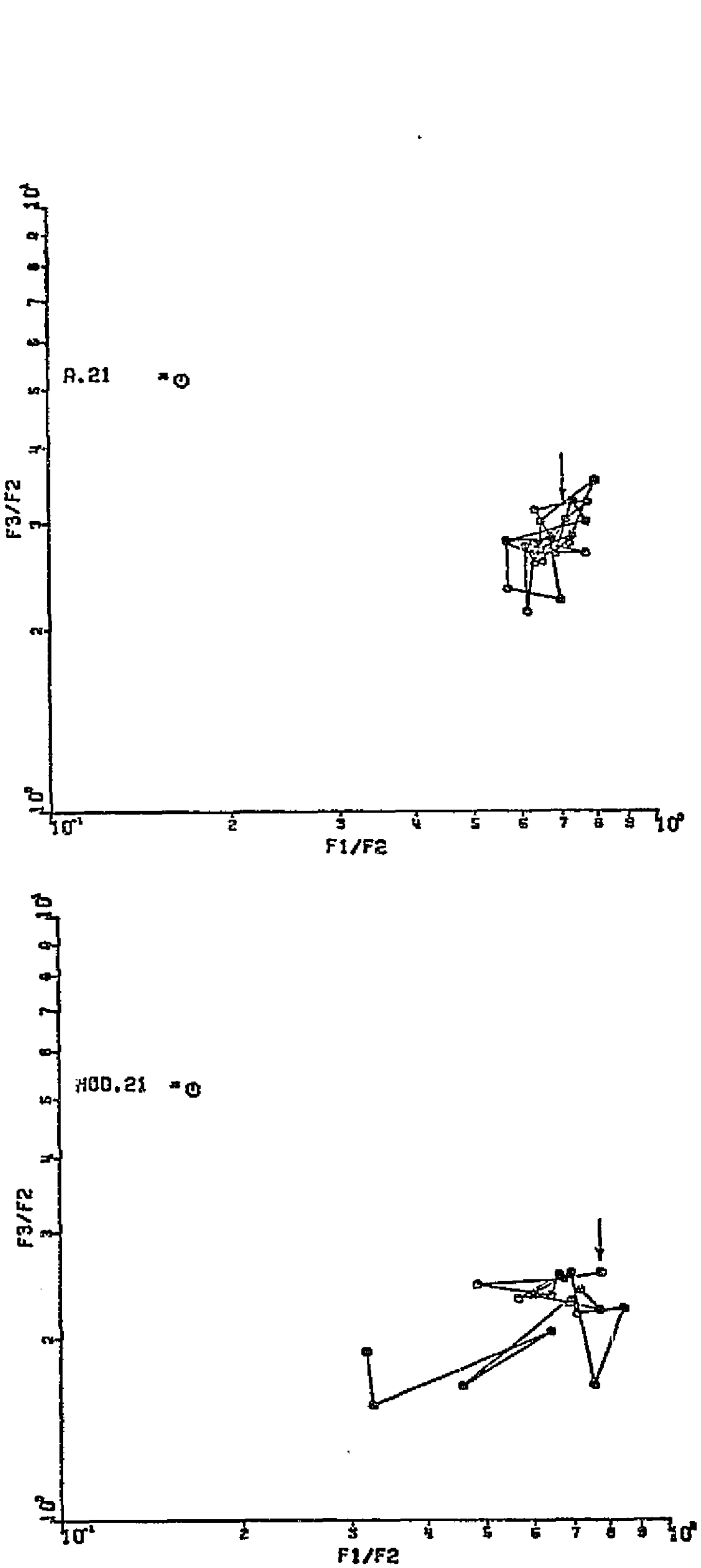


Figure 17

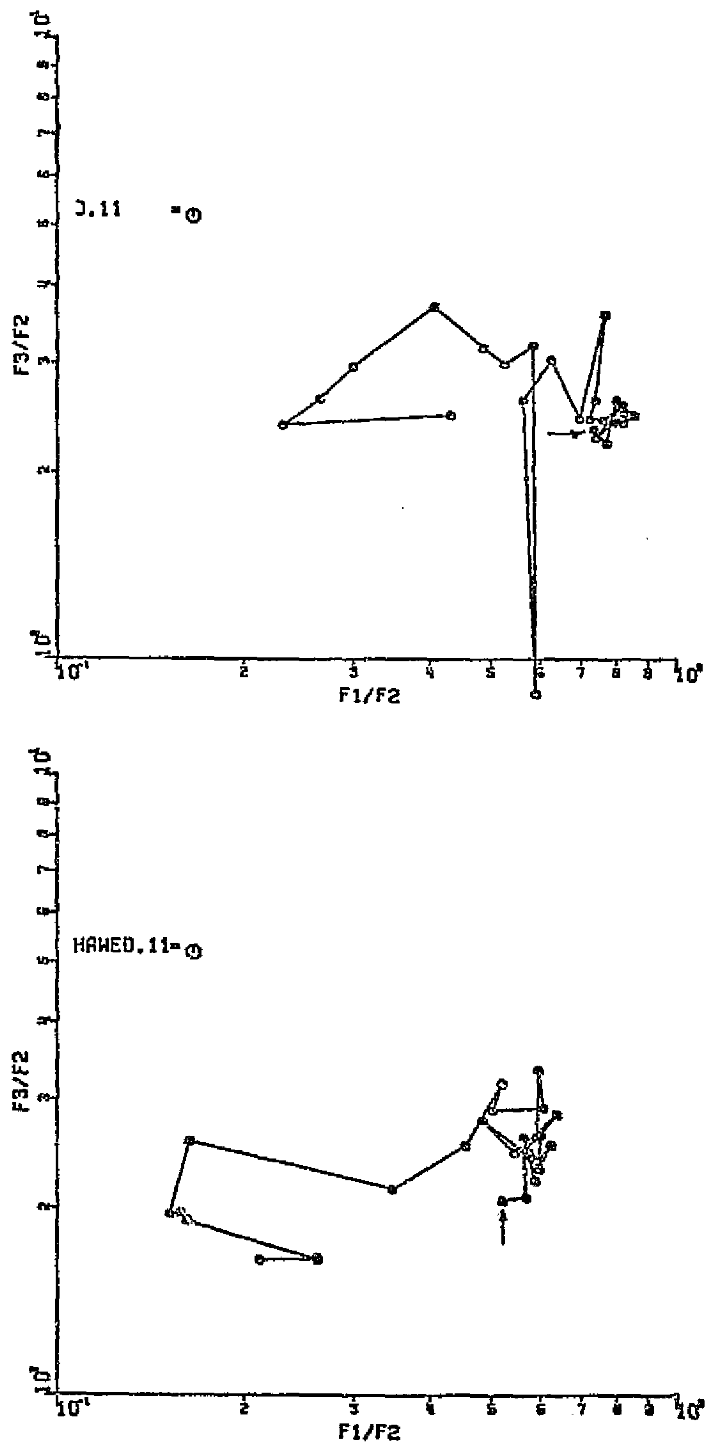


Figure 18

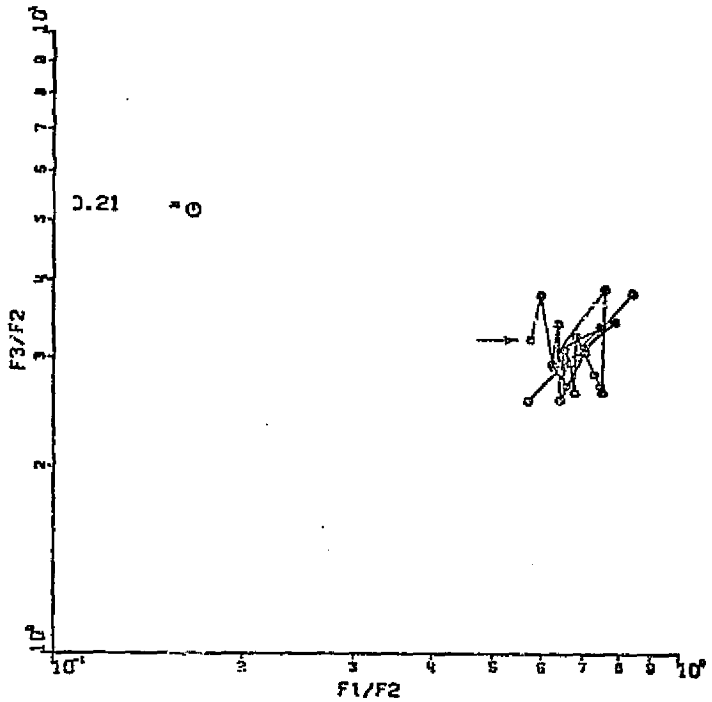


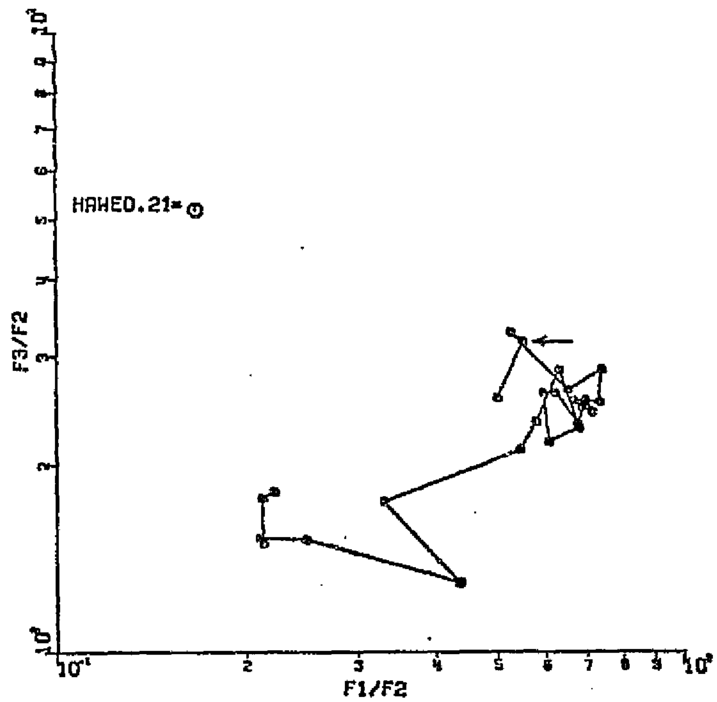


Figure 19

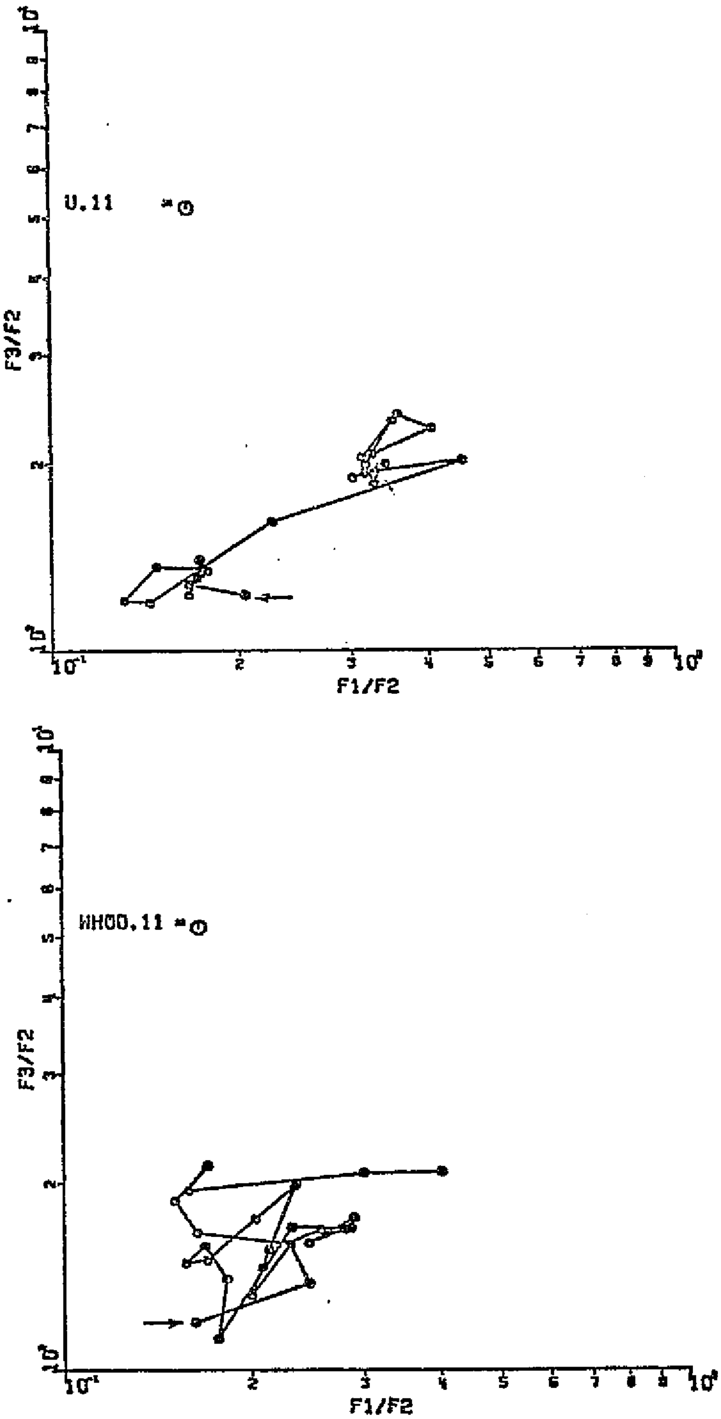


Figure 20

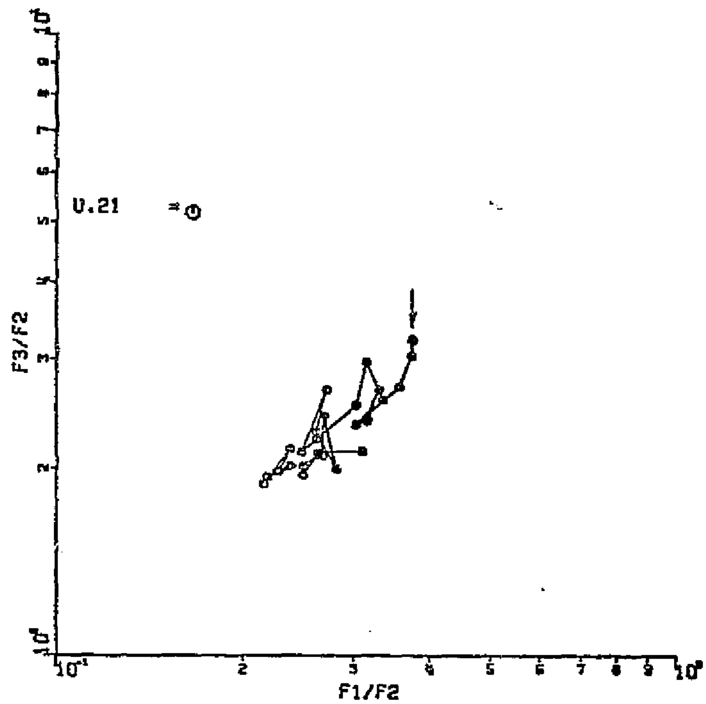


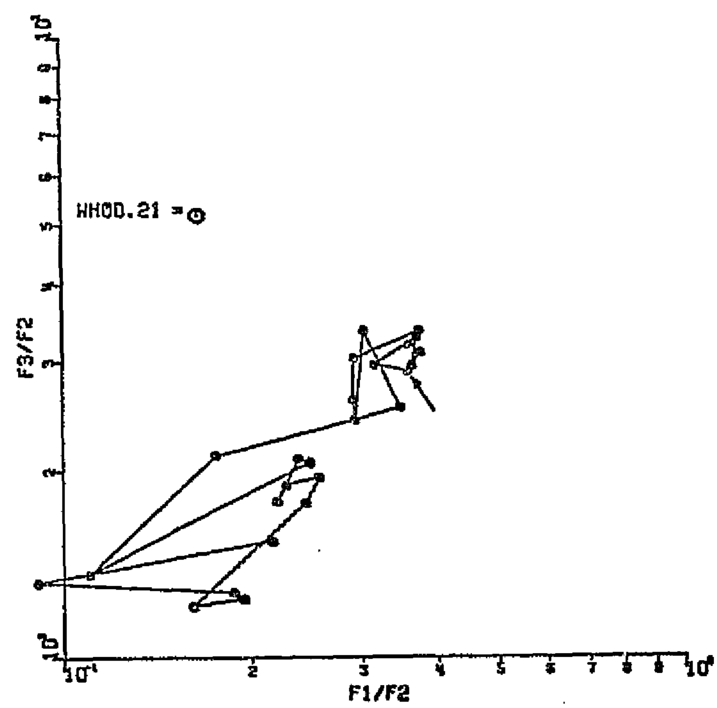


Figure 21

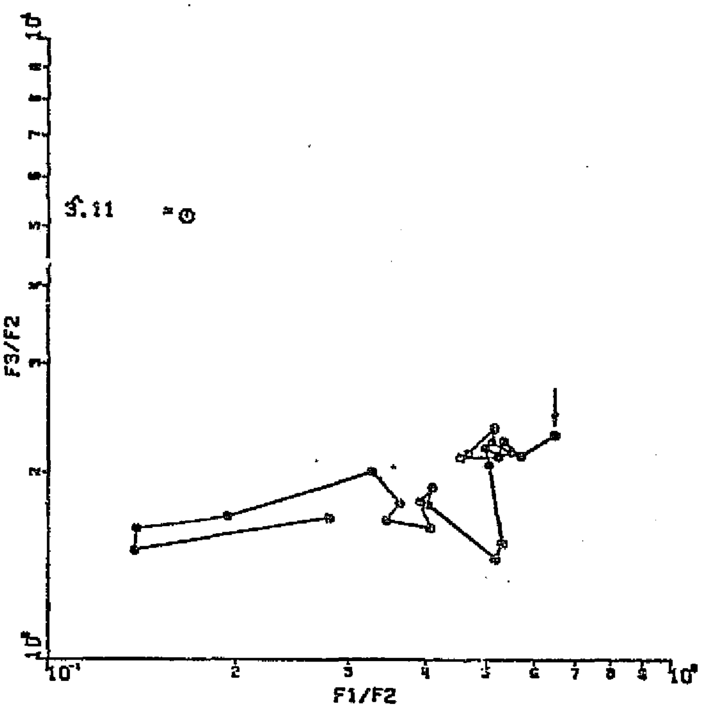


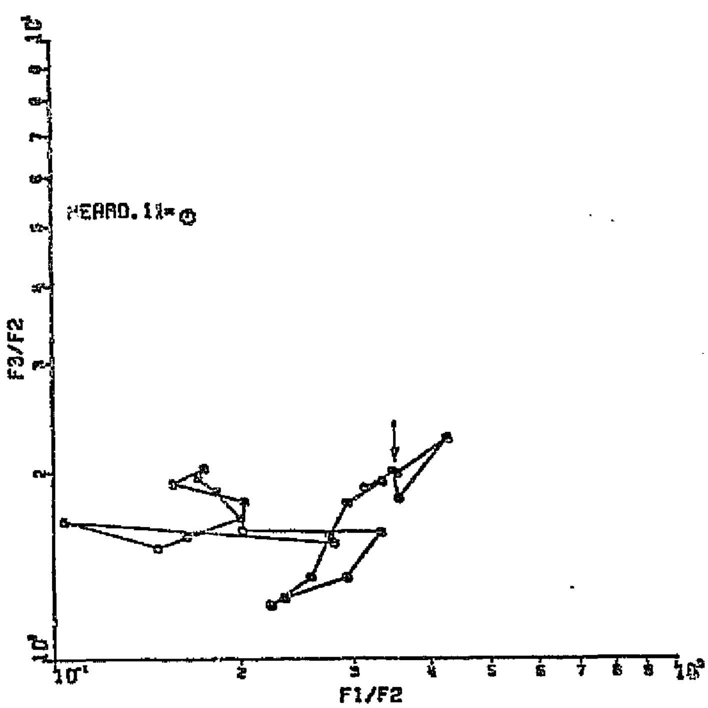


Figure 22

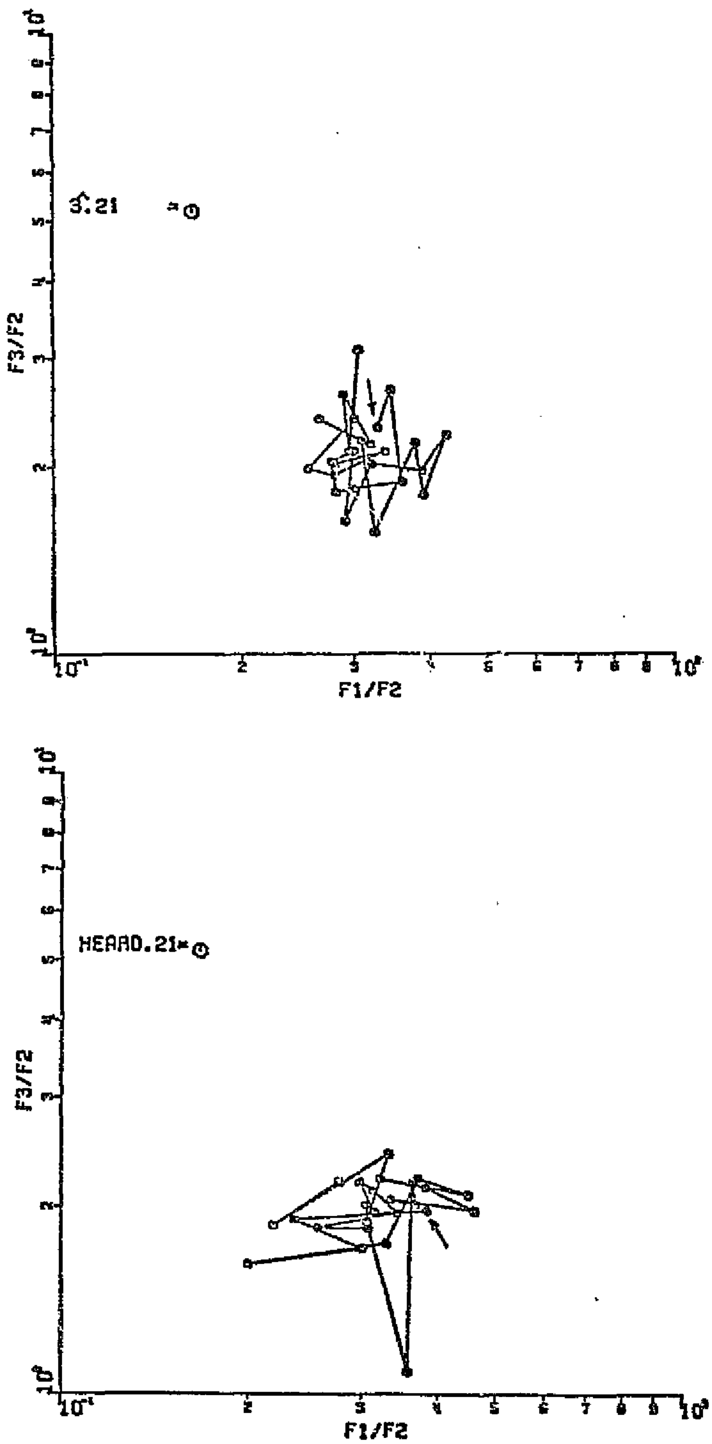


Figure 23

## 5. CONCLUSIONS AND RECOMMENDATIONS

The overall conclusion of this investigation is that the quantizer achieved consistent separation with the vowels tested, particularly in the F1/F2 axis of the formant space.

It was found that eight equally-spaced positive and negative quantizer levels yielded results which were close to thirty-two such levels, but represented some improvement over four levels. Thus, it appears that eight levels on either side of the abscissa are quite adequate for processing speech data. Similarly, it was found that setting the maximum quantizer level to the absolute value of the average of the previous block of processed data gave better results than using the peak of the waveform in the previous data block.

Although the performance of the quantizer was reasonably close to the ideal formant regions shown in Figure 7, there are several areas of investigation which, in our opinion, require further attention. These are listed below.

Filter settings: The formant filters were set to encompass the full variation of formant frequencies listed in Table 3 for men, women, and children. It is likely that improved performance could be obtained if the filters were set in an adaptive way to correspond with some (as yet unidentified) characteristics of the input speech.

Computation Interval for Formant Ratios: We feel that a more meaningful approach should be developed to designate the intervals in which the formant ratios are computed. To this effect, we recommend that a procedure to detect the beginning and ending of pitch intervals (i.e., sound bursts) in the input signals be developed. Computation of the formant ratios could then be keyed to these intervals.

Setting of Formant Levels: The maximum (and by symmetry the minimum) formant levels were set independently for each formant. It appears worthwhile to investigate the effects of using one of the formants as a normalization factor to set the levels for the remaining formants. This approach would thus take into account differences in amplitudes between the three formant signals.

It would be of value to incorporate the above features in the existing software system and reprocess the data listed in this report. The objectives of this experiment would be to ascertain whether these changes could improve separation in the F3/F2 axis and also reduce the trajectory scatters for speaker 1.

One of the most time-consuming factors in this investigation was to record, digitize, and preprocess (i.e., reconstruct) speech signals. The quantizer functions discussed in this report could be incorporated in a microprocessor system. Development of such a system would allow on-line

processing of many more speech samples while maintaining the versatility of a prototype in which changes can be made easily by modifying the software. A future task in this area should at least include a definition and cost of such a prototype system for use in further experiments with the speech quantization approach.

# REFERENCES


1. Lokerson, D. C. and H. G. Holby, "Techniques for Decoding Speech Phonemes and Sounds: A Concept," NASA Tech Briefs, B 73-10210, May, 1975.

2. Stearns, Samuel D. Digital Signal Analysis, Hyden Book Co., Rochelle Park, New Jersey, 1975.

3. White, George M. "Speech Recognition: A Tutorial Overview," Computer, pp. 49-52, May, 1976.

4. Chapanis, A. "Interactive Human Communication," Scientific American, Vol. 232(3), pp. 36-42, 1975.

5. Yasaki, Edward K. "Voice Recognition Comes of Age," Datamation, pp. 65-68, August, 1976.

6. Schroeder, Manfred R. "Models of Hearing," Proc. of the IEEE, Vol. 63, No. 9, pp. 1332-1350, September, 1975.

7. Flanagan, James L. "Computers that Talk and Listen: Man-Machine Communication by Voice," Proc. of the IEEE, Vol. 64, No. 4, pp. 405-415, April, 1976.

8. Rabiner, Lawrence R. "Scanning the Issue," Proc. of the IEEE, Vol. 64, No. 4, pp. 403-404, April, 1976.

9. Martin, Thomas B. "Practical Applications of Voice Input to Machines," Proc. of the IEEE, Vol. 64, No. 4, pp. 487-501, April, 1976.

10. Reddy, D. R. "Speech Recognition by Machine: A Review," Proc. of the IEEE, Vol. 64, No. 4, pp. 501-531, April, 1976.

11. Rabiner, Lawrence R. and Marvin R. Sambur, "Some Preliminary Experiments in the Recognition of Connected Digits," IEEE Trans. on Acoustics, Speech and Signal Proc., Vol. ASSP-24, No. 2, pp. 170-182, April, 1976.

12. Makhoul, J. "Linear Prediction: A Tutorial Review," Proc. of the IEEE, Vol. 63, No. 4, pp. 561-580, April, 1975.

13. Helmholtz, H. On the Sensation of Tone, New York, Dover, 1954.

14. Schafer, Ronald W. and Lawrence R. Rabiner, "Digital Representations of Speech Signals," Proc. of the IEEE, Vol. 63, No. 4, pp. 662-677, April, 1975.

# APPENDIX

## Computer Printouts of Processing Results

The following data were generated by the procedure described in Section 4. Speech signals were sampled at 11 KHz and reconstructed to an effective sampling rate of 100 KHz. Eight positive and eight negative levels were used in each of the three quantizers. The quantization results were printed out every 16 blocks of the reconstructed data, with each block containing 128 samples. The maximum positive quantizer levels for each 16-block data segment were set to the absolute value of the data average in the previous 16-block segment. Each formant was scaled separately, and the minimum quantizer levels were set equal to the negative of their respective maximum levels.

# APPENDIX A

## SPEECH RESULTS

### 1.11

| | RATIOS | | COUNTS | | |
|---|---|---|---|---|---|
| Blk | F1/F2 | F3/F2 | F1 | F2 | F3 |
| 16 | 0.109 | 0.929 | 90.0 | 827.0 | 768.0 |
| 32 | 0.119 | 0.947 | 82.5 | 693.0 | 656.5 |
| 48 | 0.115 | 1.027 | 81.5 | 711.5 | 731.0 |
| 64 | 0.112 | 1.081 | 77.0 | 687.0 | 742.5 |
| 80 | 0.111 | 1.094 | 82.5 | 743.0 | 812.5 |
| 96 | 0.110 | 1.125 | 75.0 | 684.5 | 770.0 |
| 112 | 0.125 | 1.241 | 81.0 | 647.5 | 803.5 |
| 128 | 0.112 | 1.313 | 76.5 | 681.5 | 895.0 |
| 144 | 0.108 | 1.243 | 77.0 | 713.5 | 887.0 |
| 160 | 0.111 | 1.072 | 85.0 | 763.0 | 818.0 |
| 176 | 0.121 | 1.073 | 90.0 | 743.0 | 797.5 |
| 192 | 0.115 | 1.066 | 87.0 | 753.5 | 803.5 |
| 208 | 0.139 | 1.336 | 82.5 | 593.0 | 792.5 |
| 224 | 0.223 | 2.017 | 78.0 | 349.0 | 704.0 |
| 240 | 0.116 | 1.483 | 70.0 | 606.0 | 899.0 |
| 256 | 0.107 | 1.434 | 72.5 | 678.5 | 973.0 |
| 272 | 0.103 | 1.243 | 67.5 | 655.5 | 815.0 |
| 288 | 0.116 | 1.391 | 78.0 | 673.0 | 936.0 |
| 304 | 0.099 | 1.185 | 69.0 | 695.5 | 824.0 |
| 320 | 0.111 | 1.250 | 74.5 | 672.0 | 840.0 |

heed.11

| Blk | RATIOS F1/F2 | RATIOS F3/F2 | COUNTS F1 | COUNTS F2 | COUNTS F3 |
|---|---|---|---|---|---|
| 16 | 0.125 | 1.274 | 82.5 | 657.5 | 837.5 |
| 32 | 0.107 | 1.055 | 82.5 | 773.0 | 815.5 |
| 48 | 0.108 | 1.180 | 75.5 | 700.0 | 826.0 |
| 64 | 0.112 | 1.141 | 82.0 | 730.0 | 833.0 |
| 80 | 0.108 | 1.128 | 80.0 | 738.0 | 832.5 |
| 96 | 0.100 | 1.010 | 78.5 | 785.0 | 792.5 |
| 112 | 0.093 | 1.011 | 76.0 | 814.5 | 823.5 |
| 128 | 0.102 | 1.034 | 75.0 | 733.0 | 758.0 |
| 144 | 0.097 | 1.101 | 73.5 | 754.0 | 830.5 |
| 160 | 0.097 | 1.038 | 72.0 | 742.0 | 770.5 |
| 176 | 0.124 | 1.151 | 84.5 | 680.5 | 783.0 |
| 192 | 0.099 | 1.062 | 76.0 | 770.5 | 818.0 |
| 208 | 0.100 | 1.066 | 72.5 | 722.0 | 770.0 |
| 224 | 0.135 | 1.080 | 74.0 | 547.0 | 591.0 |
| 240 | 0.219 | 0.956 | 47.5 | 217.0 | 207.5 |
| 256 | 0.121 | 1.559 | 41.0 | 339.0 | 528.5 |
| 272 | 0.175 | 2.148 | 64.5 | 368.0 | 790.5 |
| 288 | 0.151 | 1.906 | 60.5 | 401.0 | 764.5 |
| 304 | 0.169 | 1.992 | 66.0 | 391.0 | 779.0 |
| 320 | 0.224 | 1.449 | 126.5 | 563.5 | 816.5 |
| 336 | 0.220 | 1.453 | 135.0 | 614.5 | 893.0 |
| 352 | 0.228 | 1.277 | 120.5 | 527.5 | 673.5 |
| 368 | 0.282 | 1.322 | 133.0 | 472.0 | 624.0 |
| 384 | 0.282 | 1.549 | 118.5 | 420.0 | 650.5 |
| 400 | 0.206 | 1.389 | 89.5 | 435.5 | 605.0 |

I.21

| Blk | RATIOS F1/F2 | F3/F2 | COUNTS F1 | F2 | F3 |
|---|---|---|---|---|---|
| 16 | 0.198 | 1.331 | 96.5 | 486.5 | 647.5 |
| 32 | 0.181 | 1.398 | 96.0 | 531.0 | 742.5 |
| 48 | 0.175 | 1.417 | 90.5 | 517.0 | 732.5 |
| 64 | 0.165 | 1.286 | 90.0 | 546.5 | 703.0 |
| 80 | 0.142 | 1.137 | 90.0 | 633.0 | 720.0 |
| 96 | 0.145 | 1.167 | 83.5 | 576.5 | 673.0 |
| 112 | 0.152 | 1.173 | 89.0 | 586.0 | 687.5 |
| 128 | 0.136 | 1.146 | 82.5 | 604.5 | 693.0 |
| 144 | 0.123 | 1.146 | 77.5 | 628.0 | 720.0 |
| 160 | 0.123 | 1.106 | 78.0 | 635.0 | 702.5 |
| 176 | 0.122 | 1.039 | 84.0 | 690.0 | 717.0 |
| 192 | 0.119 | 1.115 | 79.0 | 664.5 | 741.0 |
| 208 | 0.123 | 1.086 | 77.0 | 627.5 | 681.5 |
| 224 | 0.120 | 1.112 | 75.5 | 627.0 | 697.0 |
| 240 | 0.140 | 1.049 | 87.0 | 623.5 | 654.0 |
| 256 | 0.136 | 1.053 | 93.0 | 685.0 | 721.0 |
| 272 | 0.149 | 1.065 | 91.5 | 616.0 | 656.0 |
| 288 | 0.116 | 0.966 | 90.5 | 777.0 | 750.5 |
| 304 | 0.175 | 1.039 | 83.0 | 473.5 | 492.0 |
| 320 | 0.140 | 1.111 | 82.0 | 587.0 | 652.0 |
| 336 | 0.145 | 1.187 | 82.5 | 569.0 | 675.5 |
| 352 | 0.127 | 1.159 | 79.5 | 627.0 | 727.0 |
| 368 | 0.138 | 1.240 | 75.5 | 549.0 | 680.5 |
| 384 | 0.132 | 1.279 | 77.5 | 585.5 | 749.0 |
| 400 | 0.157 | 1.414 | 78.5 | 500.5 | 707.5 |

heed.21

| | RATIØS | | CØUNTS | | |
|---|---|---|---|---|---|
| Blk | F1/F2 | F3/F2 | F1 | F2 | F3 |
| 16 | 0.215 | 1.194 | 135.5 | 630.5 | 753.0 |
| 32 | 0.153 | 1.176 | 95.0 | 620.5 | 729.5 |
| 48 | 0.214 | 1.194 | 127.0 | 594.0 | 709.0 |
| 64 | 0.185 | 1.139 | 107.0 | 577.5 | 657.5 |
| 80 | 0.280 | 1.422 | 131.5 | 469.0 | 667.0 |
| 96 | 0.149 | 1.405 | 82.5 | 554.0 | 778.5 |
| 112 | 0.111 | 1.005 | 82.5 | 745.5 | 749.5 |
| 128 | 0.117 | 1.057 | 75.0 | 642.0 | 678.5 |
| 144 | 0.119 | 1.038 | 75.5 | 632.0 | 656.0 |
| 160 | 0.128 | 1.091 | 69.0 | 538.5 | 587.5 |
| 176 | 0.133 | 1.033 | 80.5 | 606.0 | 626.0 |
| 192 | 0.195 | 1.362 | 95.5 | 490.0 | 667.5 |
| 208 | 0.183 | 1.669 | 87.0 | 476.5 | 795.5 |
| 224 | 0.204 | 1.436 | 80.0 | 393.0 | 564.5 |
| 240 | 0.123 | 1.112 | 79.5 | 646.5 | 719.0 |
| 256 | 0.136 | 1.045 | 74.0 | 546.0 | 570.5 |
| 272 | 0.110 | 1.127 | 73.0 | 663.0 | 747.0 |
| 288 | 0.114 | 1.095 | 69.5 | 612.0 | 670.0 |
| 304 | 0.140 | 1.028 | 79.5 | 569.0 | 585.0 |
| 320 | 0.150 | 0.992 | 68.0 | 453.5 | 450.0 |
| 336 | 0.143 | 1.133 | 83.0 | 581.5 | 659.0 |
| 352 | 0.164 | 1.056 | 93.0 | 566.0 | 597.5 |
| 368 | 0.144 | 1.087 | 85.0 | 589.5 | 640.5 |
| 384 | 0.142 | 1.143 | 60.0 | 423.0 | 483.5 |
| 400 | 0.140 | 1.254 | 58.5 | 418.0 | 524.0 |

ae.11

| Blk | RATIOS F1/F2 | F3/F2 | COUNTS F1 | F2 | F3 |
|---|---|---|---|---|---|
| 16 | 0.530 | 1.999 | 184.5 | 348.0 | 695.5 |
| 32 | 0.402 | 1.741 | 157.0 | 390.5 | 680.0 |
| 48 | 0.347 | 1.778 | 123.5 | 356.0 | 633.0 |
| 64 | 0.324 | 1.753 | 116.0 | 358.5 | 628.5 |
| 80 | 0.360 | 1.870 | 123.5 | 343.0 | 641.5 |
| 96 | 0.362 | 1.851 | 123.0 | 340.0 | 629.5 |
| 112 | 0.405 | 2.035 | 135.0 | 333.0 | 677.5 |
| 128 | 0.433 | 2.093 | 139.5 | 322.0 | 674.0 |
| 144 | 0.453 | 2.244 | 141.0 | 311.5 | 699.0 |
| 160 | 0.470 | 2.214 | 139.5 | 297.0 | 657.5 |
| 176 | 0.604 | 2.246 | 172.0 | 285.0 | 640.0 |
| 192 | 0.633 | 2.230 | 174.5 | 275.5 | 614.5 |
| 208 | 0.548 | 2.420 | 160.5 | 293.0 | 709.0 |
| 224 | 0.607 | 2.342 | 166.0 | 273.5 | 640.5 |
| 240 | 0.617 | 2.203 | 171.5 | 278.0 | 612.5 |
| 256 | 0.629 | 2.280 | 176.0 | 280.0 | 638.5 |
| 272 | 0.663 | 2.390 | 193.5 | 292.0 | 698.0 |
| 288 | 0.542 | 2.130 | 162.0 | 299.0 | 637.0 |
| 304 | 0.452 | 2.118 | 138.0 | 305.0 | 646.0 |
| 320 | 0.394 | 1.885 | 140.0 | 355.5 | 670.0 |
| 336 | 0.405 | 1.885 | 130.5 | 322.5 | 608.0 |
| 352 | 0.376 | 2.040 | 126.0 | 335.0 | 683.5 |
| 368 | 0.429 | 2.288 | 126.0 | 293.5 | 671.5 |
| 384 | 0.370 | 2.532 | 107.0 | 289.5 | 733.0 |
| 400 | 0.278 | 1.704 | 122.0 | 439.5 | 749.0 |

had.11

| Blk | RATIOS F1/F2 | RATIOS F3/F2 | COUNTS F1 | COUNTS F2 | COUNTS F3 |
|---|---|---|---|---|---|
| 16 | 0.440 | 1.962 | 160.0 | 364.0 | 714.0 |
| 32 | 0.421 | 1.869 | 167.0 | 396.5 | 741.0 |
| 48 | 0.448 | 1.922 | 172.5 | 385.0 | 740.0 |
| 64 | 0.444 | 1.962 | 165.5 | 373.0 | 732.0 |
| 80 | 0.417 | 1.921 | 162.0 | 388.5 | 746.5 |
| 96 | 0.419 | 1.793 | 170.0 | 405.5 | 727.0 |
| 112 | 0.396 | 1.651 | 173.0 | 437.0 | 721.5 |
| 128 | 0.412 | 1.819 | 167.0 | 405.5 | 737.5 |
| 144 | 0.463 | 1.973 | 171.0 | 369.5 | 729.0 |
| 160 | 0.505 | 2.305 | 156.5 | 310.0 | 714.5 |
| 176 | 0.631 | 2.519 | 179.0 | 283.5 | 714.0 |
| 192 | 0.642 | 2.408 | 173.0 | 269.5 | 649.0 |
| 208 | 0.670 | 2.179 | 205.5 | 306.5 | 668.0 |
| 224 | 0.672 | 2.076 | 199.5 | 297.0 | 616.5 |
| 240 | 0.703 | 2.113 | 196.0 | 279.0 | 589.5 |
| 256 | 0.672 | 2.458 | 170.0 | 253.0 | 622.0 |
| 272 | 0.644 | 2.587 | 96.0 | 149.0 | 385.5 |
| 288 | 0.191 | 2.371 | 26.0 | 136.0 | 322.5 |
| 304 | 0.167 | 1.974 | 63.5 | 380.0 | 750.0 |
| 320 | 0.163 | 1.865 | 67.0 | 411.0 | 766.5 |
| 336 | 0.172 | 2.099 | 65.5 | 380.5 | 798.5 |
| 352 | 0.212 | 1.593 | 111.0 | 522.5 | 832.5 |
| 368 | 0.219 | 1.488 | 127.5 | 583.5 | 868.5 |
| 384 | 0.248 | 1.497 | 129.5 | 522.0 | 781.5 |
| 400 | 0.294 | 1.506 | 135.5 | 461.5 | 695.0 |

ae.21

| Blk | RATIOS F1/F2 | RATIOS F3/F2 | COUNTS F1 | COUNTS F2 | COUNTS F3 |
|---|---|---|---|---|---|
| 16 | 0.318 | 1.453 | 140.0 | 440.0 | 639.5 |
| 32 | 0.327 | 1.186 | 137.0 | 418.5 | 496.5 |
| 48 | 0.292 | 1.268 | 148.0 | 506.5 | 642.0 |
| 64 | 0.322 | 1.285 | 156.5 | 486.5 | 625.0 |
| 80 | 0.382 | 1.355 | 159.0 | 416.5 | 564.5 |
| 96 | 0.394 | 1.445 | 160.5 | 407.5 | 589.0 |
| 112 | 0.361 | 1.510 | 163.5 | 453.0 | 684.0 |
| 128 | 0.446 | 1.523 | 178.5 | 400.0 | 609.0 |
| 144 | 0.422 | 1.481 | 148.0 | 350.5 | 519.0 |
| 160 | 0.406 | 1.653 | 174.0 | 428.5 | 708.5 |
| 176 | 0.528 | 1.717 | 165.0 | 312.5 | 536.5 |
| 192 | 0.552 | 1.448 | 170.5 | 309.0 | 447.5 |
| 208 | 0.412 | 2.120 | 154.0 | 374.0 | 793.0 |
| 224 | 0.416 | 1.601 | 142.5 | 342.5 | 548.5 |
| 240 | 0.349 | 1.376 | 152.5 | 436.5 | 600.5 |
| 256 | 0.373 | 1.407 | 175.0 | 469.5 | 660.5 |
| 272 | 0.429 | 1.416 | 172.0 | 400.5 | 567.0 |
| 288 | 0.351 | 1.675 | 142.0 | 404.5 | 677.5 |
| 304 | 0.456 | 1.425 | 171.5 | 376.5 | 536.5 |
| 320 | 0.519 | 1.583 | 160.5 | 309.0 | 489.0 |
| 336 | 0.406 | 1.818 | 140.5 | 346.0 | 629.0 |
| 352 | 0.346 | 1.783 | 141.5 | 408.5 | 728.5 |
| 368 | 0.340 | 1.458 | 153.0 | 449.5 | 655.5 |
| 384 | 0.579 | 1.937 | 194.0 | 335.0 | 649.0 |
| 400 | 0.286 | 1.524 | 113.0 | 395.0 | 602.0 |

had.21

| Blk | RATIOS | | COUNTS | | |
|---|---|---|---|---|---|
| | F1/F2 | F3/F2 | F1 | F2 | F3 |
| 16 | 0.359 | 1.823 | 126.0 | 351.0 | 640.0 |
| 32 | 0.330 | 1.644 | 134.0 | 405.5 | 666.5 |
| 48 | 0.416 | 1.492 | 150.0 | 360.5 | 538.0 |
| 64 | 0.434 | 1.816 | 143.5 | 331.0 | 601.0 |
| 80 | 0.371 | 1.569 | 149.5 | 403.0 | 632.5 |
| 96 | 0.407 | 1.441 | 160.0 | 393.0 | 566.5 |
| 112 | 0.418 | 1.351 | 166.0 | 397.0 | 536.5 |
| 128 | 0.366 | 1.284 | 153.5 | 419.0 | 538.0 |
| 144 | 0.419 | 1.445 | 177.0 | 422.5 | 610.5 |
| 160 | 0.552 | 1.824 | 179.0 | 324.5 | 592.0 |
| 176 | 0.468 | 1.565 | 180.5 | 385.5 | 603.5 |
| 192 | 0.373 | 1.508 | 165.5 | 444.0 | 669.5 |
| 208 | 0.394 | 1.682 | 155.0 | 393.0 | 661.0 |
| 224 | 0.382 | 1.596 | 146.5 | 384.0 | 613.0 |
| 240 | 0.548 | 1.369 | 189.5 | 345.5 | 473.0 |
| 256 | 0.424 | 1.410 | 172.5 | 406.5 | 573.0 |
| 272 | 0.357 | 1.468 | 142.0 | 397.5 | 583.5 |
| 288 | 0.373 | 2.145 | 128.5 | 344.5 | 739.0 |
| 304 | 0.197 | 1.863 | 68.5 | 347.0 | 646.5 |
| 320 | 0.213 | 1.732 | 77.0 | 362.0 | 627.0 |
| 336 | 0.194 | 1.876 | 75.5 | 388.5 | 729.0 |
| 352 | 0.194 | 1.966 | 74.5 | 385.0 | 757.0 |
| 368 | 0.185 | 1.899 | 76.5 | 414.0 | 786.0 |
| 384 | 0.185 | 1.861 | 78.5 | 425.0 | 791.0 |
| 400 | 0.225 | 1.864 | 82.0 | 365.0 | 680.5 |

a.11

| Blk | RATIOS F1/F2 | RATIOS F3/F2 | COUNTS F1 | COUNTS F2 | COUNTS F3 |
|---|---|---|---|---|---|
| 16 | 0.695 | 2.446 | 213.5 | 307.0 | 751.0 |
| 32 | 0.667 | 2.207 | 206.0 | 309.0 | 682.0 |
| 48 | 0.726 | 2.520 | 223.0 | 307.0 | 773.5 |
| 64 | 0.765 | 2.240 | 234.0 | 306.0 | 685.5 |
| 80 | 0.778 | 2.343 | 233.5 | 300.0 | 703.0 |
| 96 | 0.743 | 2.372 | 223.0 | 300.0 | 711.5 |
| 112 | 0.706 | 2.635 | 208.5 | 295.5 | 778.5 |
| 128 | 0.721 | 2.515 | 214.0 | 297.0 | 747.0 |
| 144 | 0.746 | 2.589 | 217.0 | 291.0 | 753.5 |
| 160 | 0.700 | 2.243 | 203.0 | 290.0 | 650.5 |
| 176 | 0.680 | 2.552 | 198.0 | 291.0 | 742.5 |
| 192 | 0.656 | 2.623 | 196.5 | 299.5 | 785.5 |
| 208 | 0.570 | 2.237 | 182.5 | 320.0 | 716.0 |
| 224 | 0.603 | 2.305 | 186.5 | 309.5 | 713.5 |
| 240 | 0.600 | 2.285 | 195.5 | 326.0 | 745.0 |
| 256 | 0.614 | 2.401 | 190.5 | 310.5 | 745.5 |
| 272 | 0.631 | 2.320 | 179.5 | 284.5 | 660.0 |
| 288 | 0.596 | 2.794 | 161.0 | 270.0 | 754.5 |
| 304 | 0.481 | 2.453 | 143.0 | 297.0 | 728.5 |
| 320 | 0.441 | 2.412 | 139.5 | 316.5 | 763.5 |
| 336 | 0.471 | 2.385 | 139.0 | 295.0 | 703.5 |
| 352 | 0.508 | 2.652 | 144.5 | 284.5 | 754.5 |
| 368 | 0.329 | 2.616 | 90.5 | 275.0 | 719.5 |
| 384 | 0.239 | 2.685 | 68.5 | 287.0 | 770.5 |
| 400 | 0.427 | 2.271 | 166.0 | 389.0 | 883.5 |

hod.11

| Blk | RATIOS F1/F2 | F3/F2 | COUNTS F1 | F2 | F3 |
|---|---|---|---|---|---|
| 16 | 0.538 | 2.065 | 173.5 | 322.5 | 666.0 |
| 32 | 0.638 | 2.038 | 208.0 | 326.0 | 664.5 |
| 48 | 0.677 | 2.036 | 216.0 | 319.0 | 649.5 |
| 64 | 0.652 | 2.400 | 203.0 | 311.5 | 747.5 |
| 80 | 0.700 | 1.902 | 228.0 | 325.5 | 619.0 |
| 96 | 0.728 | 2.092 | 222.5 | 305.5 | 639.0 |
| 112 | 0.712 | 2.747 | 205.0 | 288.0 | 791.0 |
| 128 | 0.739 | 2.615 | 211.0 | 285.5 | 746.5 |
| 144 | 0.676 | 2.631 | 187.0 | 276.5 | 727.5 |
| 160 | 0.650 | 2.608 | 185.0 | 284.5 | 742.0 |
| 176 | 0.647 | 2.848 | 168.0 | 259.5 | 739.0 |
| 192 | 0.687 | 2.424 | 186.5 | 271.5 | 658.0 |
| 208 | 0.569 | 2.445 | 167.0 | 293.5 | 717.5 |
| 224 | 0.599 | 2.580 | 172.0 | 287.0 | 740.5 |
| 240 | 0.575 | 2.551 | 162.0 | 281.5 | 718.0 |
| 256 | 0.567 | 2.457 | 162.5 | 286.5 | 704.0 |
| 272 | 0.660 | 2.774 | 176.5 | 267.5 | 742.0 |
| 288 | 0.635 | 2.914 | 163.0 | 256.5 | 747.5 |
| 304 | 0.610 | 2.461 | 150.0 | 246.0 | 605.5 |
| 320 | 0.190 | 2.231 | 46.5 | 244.5 | 545.5 |
| 336 | 0.147 | 2.112 | 61.0 | 414.5 | 875.5 |
| 352 | 0.218 | 1.665 | 95.5 | 437.5 | 728.5 |
| 368 | 0.239 | 2.113 | 89.5 | 375.0 | 792.5 |
| 384 | 0.167 | 2.148 | 61.0 | 365.5 | 785.0 |
| 407 | 0.377 | 2.434 | 135.0 | 358.0 | 871.5 |

a.21

| Blk | RATIOS F1/F2 | F3/F2 | COUNTS F1 | F2 | F3 |
|---|---|---|---|---|---|
| 16 | 0.714 | 3.040 | 188.5 | 264.0 | 802.5 |
| 32 | 0.651 | 2.593 | 197.5 | 303.5 | 787.0 |
| 48 | 0.632 | 2.574 | 186.0 | 294.5 | 758.0 |
| 64 | 0.609 | 2.743 | 161.0 | 264.5 | 725.5 |
| 80 | 0.614 | 2.138 | 171.5 | 279.5 | 597.5 |
| 96 | 0.631 | 2.652 | 166.5 | 264.0 | 700.0 |
| 112 | 0.568 | 2.777 | 149.0 | 262.5 | 729.0 |
| 128 | 0.570 | 2.334 | 163.0 | 286.0 | 667.5 |
| 144 | 0.698 | 2.233 | 205.5 | 294.5 | 657.5 |
| 160 | 0.670 | 2.839 | 170.5 | 254.5 | 722.5 |
| 176 | 0.630 | 2.779 | 165.5 | 262.5 | 729.5 |
| 192 | 0.768 | 2.674 | 204.0 | 265.5 | 710.0 |
| 208 | 0.616 | 2.657 | 177.0 | 287.5 | 764.0 |
| 224 | 0.774 | 3.253 | 171.0 | 221.0 | 719.0 |
| 240 | 0.634 | 3.150 | 180.0 | 284.0 | 894.5 |
| 256 | 0.675 | 2.811 | 180.0 | 266.5 | 749.0 |
| 272 | 0.567 | 2.800 | 165.5 | 292.0 | 817.5 |
| 288 | 0.770 | 3.022 | 214.0 | 278.0 | 840.0 |
| 304 | 0.732 | 3.270 | 189.5 | 259.0 | 847.0 |
| 320 | 0.684 | 2.666 | 191.5 | 280.0 | 746.5 |
| 336 | 0.729 | 2.860 | 192.5 | 264.0 | 755.0 |
| 352 | 0.646 | 2.708 | 181.5 | 281.0 | 761.0 |
| 368 | 0.648 | 3.022 | 187.5 | 289.5 | 875.0 |
| 384 | 0.797 | 3.528 | 196.0 | 246.0 | 868.0 |
| 400 | 0.722 | 2.776 | 201.0 | 278.5 | 773.0 |

hod.21

| Blk | RATIOS F1/F2 | RATIOS F3/F2 | COUNTS F1 | COUNTS F2 | COUNTS F3 |
|---|---|---|---|---|---|
| 16 | 0.777 | 2.568 | 226.5 | 291.5 | 748.5 |
| 32 | 0.673 | 2.509 | 184.5 | 274.0 | 687.5 |
| 48 | 0.485 | 2.454 | 151.0 | 311.5 | 764.5 |
| 64 | 0.643 | 2.354 | 199.0 | 309.5 | 728.5 |
| 80 | 0.664 | 2.551 | 179.0 | 269.5 | 687.5 |
| 96 | 0.567 | 2.326 | 179.0 | 315.5 | 734.0 |
| 112 | 0.605 | 2.356 | 172.5 | 285.0 | 671.5 |
| 128 | 0.688 | 2.283 | 200.5 | 291.5 | 665.5 |
| 144 | 0.695 | 2.312 | 191.5 | 275.5 | 637.0 |
| 160 | 0.710 | 2.195 | 198.0 | 279.0 | 612.5 |
| 176 | 0.846 | 2.237 | 225.0 | 266.0 | 595.0 |
| 192 | 0.757 | 1.674 | 202.0 | 267.0 | 447.0 |
| 208 | 0.694 | 2.567 | 172.0 | 248.0 | 636.5 |
| 224 | 0.592 | 2.361 | 173.0 | 292.0 | 689.5 |
| 240 | 0.773 | 2.229 | 212.5 | 275.0 | 613.0 |
| 256 | 0.719 | 2.402 | 181.5 | 252.5 | 606.5 |
| 272 | 0.458 | 1.668 | 174.5 | 381.0 | 635.5 |
| 288 | 0.641 | 2.051 | 177.5 | 277.0 | 568.0 |
| 304 | 0.326 | 1.551 | 150.0 | 460.0 | 713.5 |
| 320 | 0.318 | 1.902 | 120.5 | 378.5 | 720.0 |

D.11

| Blk | RATIOS F1/F2 | RATIOS F3/F2 | COUNTS F1 | COUNTS F2 | COUNTS F3 |
|---|---|---|---|---|---|
| 16 | 0.736 | 2.342 | 240.0 | 326.0 | 763.5 |
| 32 | 0.771 | 2.230 | 251.5 | 326.0 | 727.0 |
| 48 | 0.801 | 2.614 | 248.0 | 309.5 | 809.0 |
| 64 | 0.856 | 2.468 | 260.5 | 304.5 | 751.5 |
| 80 | 0.820 | 2.404 | 248.5 | 303.0 | 728.5 |
| 96 | 0.823 | 2.484 | 249.0 | 302.5 | 751.5 |
| 112 | 0.793 | 2.408 | 241.0 | 304.0 | 732.0 |
| 128 | 0.741 | 2.270 | 236.0 | 318.5 | 723.0 |
| 144 | 0.819 | 2.569 | 242.5 | 296.0 | 760.5 |
| 160 | 0.762 | 2.429 | 222.0 | 291.5 | 708.0 |
| 176 | 0.724 | 2.434 | 206.0 | 284.5 | 692.5 |
| 192 | 0.740 | 2.612 | 202.0 | 273.0 | 713.0 |
| 208 | 0.768 | 3.596 | 156.0 | 203.0 | 730.0 |
| 224 | 0.697 | 2.442 | 150.5 | 216.0 | 527.5 |
| 240 | 0.627 | 3.035 | 163.0 | 260.0 | 789.0 |
| 256 | 0.564 | 2.612 | 177.5 | 314.5 | 821.5 |
| 272 | 0.590 | 0.878 | 154.5 | 262.0 | 230.0 |
| 288 | 0.586 | 3.204 | 150.5 | 257.0 | 823.5 |
| 304 | 0.527 | 2.989 | 149.0 | 282.5 | 844.5 |
| 320 | 0.488 | 3.175 | 128.5 | 263.5 | 836.5 |
| 336 | 0.407 | 3.709 | 97.0 | 238.5 | 884.5 |
| 352 | 0.300 | 2.964 | 84.5 | 281.5 | 834.5 |
| 368 | 0.265 | 2.627 | 77.0 | 290.5 | 763.0 |
| 384 | 0.231 | 2.381 | 77.0 | 333.0 | 793.0 |
| 400 | 0.432 | 2.471 | 150.0 | 347.0 | 857.5 |

hawed.11

| Blk | RATIØS F1/F2 | F3/F2 | COUNTS F1 | F2 | F3 |
|---|---|---|---|---|---|
| 16 | 0.522 | 2.055 | 175.5 | 336.5 | 691.5 |
| 32 | 0.569 | 2.085 | 187.0 | 328.5 | 685.0 |
| 48 | 0.564 | 2.496 | 187.5 | 332.5 | 830.0 |
| 64 | 0.601 | 2.625 | 196.5 | 327.0 | 858.5 |
| 80 | 0.597 | 2.314 | 197.5 | 331.0 | 766.0 |
| 96 | 0.624 | 2.530 | 206.0 | 330.0 | 835.0 |
| 112 | 0.594 | 2.391 | 191.5 | 322.5 | 771.0 |
| 128 | 0.564 | 2.602 | 182.0 | 322.5 | 839.0 |
| 144 | 0.589 | 2.218 | 182.5 | 310.0 | 687.5 |
| 160 | 0.579 | 2.413 | 174.0 | 300.5 | 725.0 |
| 176 | 0.485 | 2.774 | 141.5 | 291.5 | 808.5 |
| 192 | 0.545 | 2.464 | 151.0 | 277.0 | 682.5 |
| 208 | 0.640 | 2.836 | 168.0 | 262.5 | 744.5 |
| 224 | 0.592 | 2.603 | 156.5 | 264.5 | 688.5 |
| 240 | 0.597 | 3.341 | 157.5 | 264.0 | 882.0 |
| 256 | 0.607 | 2.906 | 148.5 | 244.5 | 710.5 |
| 272 | 0.504 | 2.879 | 137.0 | 272.0 | 783.0 |
| 288 | 0.521 | 3.182 | 137.5 | 264.0 | 840.0 |
| 304 | 0.456 | 2.525 | 138.5 | 304.0 | 767.5 |
| 320 | 0.348 | 2.150 | 119.5 | 343.0 | 737.5 |
| 336 | 0.164 | 2.565 | 31.0 | 189.5 | 486.0 |
| 352 | 0.152 | 1.956 | 61.0 | 402.0 | 786.5 |
| 368 | 0.158 | 1.966 | 62.5 | 394.5 | 775.5 |
| 384 | 0.162 | 1.913 | 61.5 | 378.5 | 724.0 |
| 400 | 0.262 | 1.653 | 133.5 | 510.5 | 844.0 |
| 416 | 0.262 | 1.661 | 127.5 | 486.5 | 808.0 |
| 432 | 0.212 | 1.653 | 96.5 | 454.5 | 751.5 |

).21

| | RATIOS | | COUNTS | | |
|---|---|---|---|---|---|
| Blk | F1/F2 | F3/F2 | F1 | F2 | F3 |
| 16 | 0.577 | 3.217 | 145.0 | 251.5 | 809.0 |
| 32 | 0.598 | 3.785 | 139.0 | 232.5 | 880.0 |
| 48 | 0.627 | 2.903 | 164.5 | 262.5 | 762.0 |
| 64 | 0.659 | 2.710 | 178.5 | 271.0 | 734.5 |
| 80 | 0.644 | 2.846 | 169.0 | 262:5 | 747.0 |
| 96 | 0.653 | 3.090 | 170.5 | 261.0 | 806.5 |
| 112 | 0.668 | 2.941 | 175.0 | 262.0 | 770.5 |
| 128 | 0.678 | 2.640 | 168.5 | 248.5 | 656.0 |
| 144 | 0.684 | 3.248 | 161.5 | 236.0 | 766.5 |
| 160 | 0.731 | 2.825 | 175.5 | 240.0 | 678.0 |
| 176 | 0.747 | 2.703 | 171.0 | 229.0 | 619.0 |
| 192 | 0.752 | 2.645 | 183.0 | 243.5 | 644.0 |
| 208 | 0.761 | 3.885 | 145.0 | 190.5 | 740.0 |
| 224 | 0.641 | 3.100 | 154.5 | 241.0 | 747.0 |
| 240 | 0.746 | 3.366 | 186.5 | 250.0 | 841.5 |
| 256 | 0.569 | 2.560 | 154.5 | 271.5 | 695.0 |
| 272 | 0.645 | 2.884 | 172.5 | 267.5 | 771.5 |
| 288 | 0.623 | 2.935 | 158.0 | 253.5 | 744.0 |
| 304 | 0.638 | 3.407 | 156.0 | 244.5 | 833.0 |
| 320 | 0.642 | 2.572 | 168.0 | 261.5 | 672.5 |
| 336 | 0.706 | 3.065 | 157.5 | 223.0 | 683.5 |
| 352 | 0.704 | 3.118 | 172.5 | 245.0 | 764.0 |
| 368 | 0.788 | 3.434 | 154.5 | 196.0 | 673.0 |
| 384 | 0.684 | 3.013 | 188.0 | 275.0 | 828.5 |
| 400 | 0.841 | 3.813 | 150.5 | 179.0 | 682.5 |

hawed.21

| Blk | RATIOS F1/F2 | RATIOS F3/F2 | COUNTS F1 | COUNTS F2 | COUNTS F3 |
|---|---|---|---|---|---|
| 16 | 0.501 | 2.566 | 156.5 | 312.5 | 802.0 |
| 32 | 0.551 | 3.159 | 156.0 | 283.0 | 894.0 |
| 48 | 0.526 | 3.279 | 141.5 | 269.0 | 882.0 |
| 64 | 0.652 | 2.644 | 194.0 | 297.5 | 786.5 |
| 80 | 0.739 | 2.851 | 198.0 | 268.0 | 764.0 |
| 96 | 0.732 | 2.527 | 195.0 | 266.5 | 673.5 |
| 112 | 0.666 | 2.544 | 180.5 | 271.0 | 689.5 |
| 128 | 0.687 | 2.479 | 182.0 | 265.0 | 657.0 |
| 144 | 0.713 | 2.440 | 185.5 | 260.0 | 634.5 |
| 160 | 0.696 | 2.543 | 179.5 | 258.0 | 656.0 |
| 176 | 0.677 | 2.338 | 159.0 | 235.0 | 549.5 |
| 192 | 0.622 | 2.614 | 150.0 | 241.0 | 630.0 |
| 208 | 0.595 | 2.616 | 165.0 | 277.5 | 726.0 |
| 224 | 0.607 | 2.179 | 166.5 | 274.5 | 598.0 |
| 240 | 0.680 | 2.301 | 199.0 | 292.5 | 673.0 |
| 256 | 0.631 | 2.845 | 140.0 | 222.0 | 631.5 |
| 272 | 0.579 | 2.351 | 176.5 | 305.0 | 717.0 |
| 288 | 0.545 | 2.120 | 167.5 | 307.5 | 652.0 |
| 304 | 0.330 | 1.750 | 136.0 | 412.5 | 722.0 |
| 320 | 0.436 | 1.292 | 163.5 | 375.0 | 484.5 |
| 336 | 0.249 | 1.516 | 121.0 | 486.5 | 737.5 |
| 352 | 0.210 | 1.526 | 93.0 | 443.5 | 677.0 |
| 368 | 0.213 | 1.497 | 73.5 | 345.0 | 516.5 |
| 384 | 0.212 | 1.[illegible]09 | 88.5 | 417.0 | 737.5 |
| 400 | 0.222 | 1.814 | 99.0 | 446.5 | 810.0 |

u.11

| Blk | RATIOS F1/F2 | RATIOS F3/F2 | COUNTS F1 | COUNTS F2 | COUNTS F3 |
|---|---|---|---|---|---|
| 16 | 0.204 | 1.227 | 117.5 | 575.0 | 705.5 |
| 32 | 0.166 | 1.279 | 97.5 | 586.5 | 750.0 |
| 48 | 0.173 | 1.328 | 97.5 | 562.5 | 747.0 |
| 64 | 0.166 | 1.227 | 86.5 | 521.0 | 639.5 |
| 80 | 0.171 | 1.305 | 89.0 | 519.5 | 678.0 |
| 96 | 0.173 | 1.399 | 86.5 | 499.5 | 699.0 |
| 112 | 0.178 | 1.344 | 92.5 | 520.0 | 699.0 |
| 128 | 0.166 | 1.278 | 86.5 | 520.0 | 664.5 |
| 144 | 0.174 | 1.357 | 88.5 | 509.0 | 690.5 |
| 160 | 0.147 | 1.362 | 77.0 | 523.0 | 712.5 |
| 176 | 0.130 | 1.202 | 77.0 | 590.5 | 709.5 |
| 192 | 0.143 | 1.192 | 79.5 | 557.0 | 664.0 |
| 208 | 0.226 | 1.613 | 89.0 | 393.0 | 634.0 |
| 224 | 0.455 | 2.022 | 111.5 | 245.0 | 495.5 |
| 240 | 0.316 | 1.925 | 123.5 | 391.0 | 752.5 |
| 256 | 0.303 | 1.894 | 124.5 | 411.5 | 779.5 |
| 272 | 0.342 | 1.995 | 129.0 | 377.5 | 753.0 |
| 288 | 0.335 | 1.967 | 127.0 | 379.0 | 745.5 |
| 304 | 0.328 | 1.854 | 122.5 | 373.5 | 692.5 |
| 320 | 0.314 | 2.045 | 125.0 | 397.5 | 813.0 |
| 336 | 0.351 | 2.344 | 120.0 | 341.5 | 800.5 |
| 352 | 0.318 | 1.986 | 121.5 | 381.5 | 757.5 |
| 368 | 0.326 | 2.069 | 125.5 | 385.5 | 797.5 |
| 384 | 0.406 | 2.280 | 127.0 | 313.0 | 713.5 |
| 400 | 0.358 | 2.397 | 123.0 | 343.5 | 823.5 |

whod.11

| Blk | RATIOS F1/F2 | RATIOS F3/F2 | COUNTS F1 | COUNTS F2 | COUNTS F3 |
|---|---|---|---|---|---|
| 16 | 0.163 | 1.194 | 97.5 | 596.5 | 712.5 |
| 32 | 0.246 | 1.380 | 91.5 | 371.5 | 512.5 |
| 48 | 0.230 | 1.592 | 100.0 | 434.0 | 691.0 |
| 64 | 0.200 | 1.319 | 120.0 | 601.0 | 793.0 |
| 80 | 0.236 | 2.003 | 90.0 | 381.5 | 764.0 |
| 96 | 0.213 | 1.561 | 96.0 | 450.0 | 702.5 |
| 112 | 0.208 | 1.460 | 89.5 | 430.0 | 628.0 |
| 128 | 0.234 | 1.978 | 86.5 | 370.0 | 732.0 |
| 144 | 0.203 | 1.751 | 87.5 | 430.5 | 754.0 |
| 160 | 0.170 | 1.502 | 82.5 | 485.5 | 729.0 |
| 176 | 0.157 | 1.485 | 82.5 | 525.0 | 779.5 |
| 192 | 0.169 | 1.584 | 82.5 | 488.5 | 774.0 |
| 208 | 0.183 | 1.400 | 81.0 | 443.5 | 621.0 |
| 224 | 0.177 | 1.123 | 80.5 | 454.5 | 510.5 |
| 240 | 0.232 | 1.699 | 99.0 | 427.5 | 726.5 |
| 256 | 0.281 | 1.688 | 118.0 | 420.0 | 709.0 |
| 272 | 0.246 | 1.604 | 109.0 | 443.5 | 711.5 |
| 288 | 0.290 | 1.760 | 120.5 | 415.0 | 730.5 |
| 304 | 0.286 | 1.695 | 122.5 | 429.0 | 727.0 |
| 320 | 0.256 | 1.681 | 116.5 | 455.0 | 765.0 |
| 336 | 0.228 | 1.597 | 110.0 | 482.5 | 770.5 |
| 352 | 0.164 | 1.665 | 52.0 | 317.5 | 528.5 |
| 368 | 0.151 | 1.873 | 53.0 | 350.5 | 656.5 |
| 384 | 0.171 | 2.136 | 66.5 | 389.5 | 832.0 |
| 400 | 0.159 | 1.948 | 62.5 | 393.0 | 765.5 |
| 416 | 0.301 | 2.077 | 115.0 | 382.0 | 793.5 |
| 432 | 0.402 | 2.088 | 135.0 | 336.0 | 701.5 |

u.21

| Blk | RATIOS F1/F2 | F3/F2 | COUNTS F1 | F2 | F3 |
|---|---|---|---|---|---|
| 16 | 0.375 | 3.231 | 102.5 | 273.0 | 882.0 |
| 32 | 0.374 | 3.040 | 103.5 | 276.5 | 840.5 |
| 48 | 0.357 | 2.709 | 97.5 | 273.0 | 739.5 |
| 64 | 0.302 | 2.357 | 97.0 | 321.0 | 756.5 |
| 80 | 0.315 | 2.390 | 103.0 | 327.0 | 781.5 |
| 96 | 0.330 | 2.682 | 96.5 | 292.0 | 783.0 |
| 112 | 0.335 | 2.586 | 97.5 | 291.0 | 752.5 |
| 128 | 0.315 | 2.970 | 90.0 | 285.5 | 848.0 |
| 144 | 0.303 | 2.534 | 91.0 | 300.5 | 761.5 |
| 160 | 0.261 | 2.234 | 87.5 | 335.0 | 748.5 |
| 176 | 0.247 | 2.130 | 85.0 | 343.5 | 731.5 |
| 192 | 0.271 | 2.679 | 87.5 | 322.5 | 864.0 |
| 208 | 0.260 | 2.297 | 89.0 | 342.0 | 785.5 |
| 224 | 0.281 | 1.996 | 96.0 | 342.0 | 682.5 |
| 240 | 0.268 | 2.432 | 93.0 | 347.0 | 844.0 |
| 256 | 0.267 | 2.099 | 88.0 | 329.5 | 691.5 |
| 272 | 0.218 | 1.941 | 92.0 | 422.5 | 820.0 |
| 288 | 0.215 | 1.889 | 82.5 | 384.5 | 726.5 |
| 304 | 0.237 | 2.150 | 84.5 | 356.0 | 765.5 |
| 320 | 0.227 | 1.984 | 87.5 | 385.0 | 764.0 |
| 336 | 0.236 | 2.019 | 93.5 | 397.0 | 801.5 |
| 352 | 0.248 | 2.017 | 90.0 | 362.5 | 731.0 |
| 368 | 0.248 | 1.956 | 102.0 | 412.0 | 806.0 |
| 384 | 0.262 | 2.119 | 95.0 | 362.0 | 767.0 |
| 400 | 0.310 | 2.130 | 111.0 | 357.5 | 761.5 |

whod.21

| Blk | RATIOS F1/F2 | RATIOS F3/F2 | COUNTS F1 | COUNTS F2 | COUNTS F3 |
|---|---|---|---|---|---|
| 16 | 0.360 | 2.891 | 94.5 | 262.5 | 759.0 |
| 32 | 0.316 | 2.956 | 83.5 | 264.0 | 780.5 |
| 48 | 0.372 | 3.279 | 90.0 | 242.0 | 793.5 |
| 64 | 0.365 | 2.949 | 96.5 | 264.5 | 780.0 |
| 80 | 0.377 | 3.099 | 98.5 | 261.5 | 810.5 |
| 96 | 0.361 | 3.189 | 91.5 | 253.5 | 808.5 |
| 112 | 0.376 | 3.357 | 87.5 | 232.5 | 780.5 |
| 128 | 0.293 | 3.035 | 83.5 | 285.0 | 865.0 |
| 144 | 0.292 | 2.596 | 85.5 | 293.0 | 760.5 |
| 160 | 0.294 | 2.414 | 85.5 | 291.0 | 702.5 |
| 176 | 0.304 | 3.360 | 88.5 | 291.5 | 979.5 |
| 192 | 0.349 | 2.530 | 99.0 | 284.0 | 718.5 |
| 208 | 0.177 | 2.117 | 66.0 | 372.5 | 788.5 |
| 224 | 0.110 | 1.361 | 34.0 | 309.0 | 420.5 |
| 240 | 0.248 | 2.059 | 78.0 | 314.5 | 647.5 |
| 256 | 0.238 | 2.083 | 91.5 | 384.0 | 800.0 |
| 272 | 0.220 | 1.781 | 93.0 | 422.0 | 751.5 |
| 288 | 0.227 | 1.893 | 91.5 | 403.5 | 764.0 |
| 304 | 0.257 | 1.950 | 106.0 | 413.0 | 805.5 |
| 320 | 0.244 | 1.773 | 109.0 | 447.5 | 793.5 |
| 336 | 0.162 | 1.210 | 108.0 | 667.0 | 807.0 |
| 352 | 0.195 | 1.242 | 100.0 | 513.0 | 637.0 |
| 368 | 0.188 | 1.271 | 108.5 | 576.5 | 732.5 |
| 384 | 0.091 | 1.319 | 45.5 | 500.5 | 660.0 |
| 400 | 0.216 | 1.537 | 99.0 | 457.5 | 703.0 |

5.11

| Blk | RATIOS F1/F2 | RATIOS F3/F2 | COUNTS F1 | COUNTS F2 | COUNTS F3 |
|---|---|---|---|---|---|
| 16 | 0.647 | 2.300 | 194.0 | 300.0 | 690.0 |
| 32 | 0.569 | 2.126 | 175.5 | 308.5 | 656.0 |
| 48 | 0.533 | 2.242 | 165.5 | 310.5 | 696.0 |
| 64 | 0.521 | 2.115 | 161.0 | 309.0 | 653.5 |
| 80 | 0.454 | 2.111 | 144.5 | 318.5 | 672.5 |
| 96 | 0.467 | 2.142 | 148.5 | 318.0 | 681.0 |
| 112 | 0.515 | 2.355 | 159.5 | 310.0 | 730.0 |
| 128 | 0.510 | 2.240 | 155.0 | 304.0 | 681.0 |
| 144 | 0.548 | 2.153 | 166.5 | 304.0 | 654.5 |
| 160 | 0.523 | 2.122 | 156.5 | 299.5 | 635.5 |
| 176 | 0.498 | 2.191 | 150.0 | 301.5 | 660.5 |
| 192 | 0.505 | 2.058 | 148.5 | 294.0 | 605.0 |
| 208 | 0.530 | 1.539 | 148.5 | 280.0 | 431.0 |
| 224 | 0.516 | 1.451 | 151.5 | 293.5 | 426.0 |
| 240 | 0.402 | 1.775 | 151.5 | 377.0 | 669.0 |
| 256 | 0.409 | 1.893 | 145.5 | 355.5 | 673.0 |
| 272 | 0.391 | 1.794 | 148.0 | 378.5 | 679.0 |
| 288 | 0.405 | 1.627 | 158.5 | 391.5 | 637.0 |
| 304 | 0.344 | 1.670 | 138.0 | 401.0 | 669.5 |
| 320 | 0.362 | 1.782 | 139.5 | 385.0 | 686.0 |
| 336 | 0.326 | 2.004 | 112.0 | 343.5 | 688.5 |
| 352 | 0.194 | 1.698 | 77.5 | 399.5 | 678.5 |
| 368 | 0.138 | 1.623 | 60.0 | 436.0 | 707.5 |
| 384 | 0.137 | 1.494 | 64.5 | 472.5 | 706.0 |
| 400 | 0.279 | 1.689 | 122.0 | 437.5 | 739.0 |

heard.11

| Blk | RATIOS F1/F2 | F3/F2 | COUNTS F1 | F2 | F3 |
|---|---|---|---|---|---|
| 16 | 0.347 | 2.003 | 121.0 | 348.5 | 698.0 |
| 32 | 0.355 | 1.811 | 123.0 | 346.0 | 626.5 |
| 48 | 0.426 | 2.264 | 131.5 | 309.0 | 699.5 |
| 64 | 0.353 | 1.989 | 107.5 | 304.5 | 605.5 |
| 80 | 0.348 | 1.997 | 105.0 | 302.0 | 603.0 |
| 96 | 0.313 | 1.880 | 99.0 | 316.5 | 595.0 |
| 112 | 0.334 | 1.927 | 109.5 | 328.0 | 632.0 |
| 128 | 0.294 | 1.781 | 109.0 | 370.5 | 660.0 |
| 144 | 0.276 | 1.582 | 112.5 | 407.5 | 644.5 |
| 160 | 0.258 | 1.354 | 123.0 | 476.5 | 645.0 |
| 176 | 0.223 | 1.220 | 116.5 | 522.5 | 637.5 |
| 192 | 0.234 | 1.252 | 114.0 | 486.5 | 609.0 |
| 208 | 0.293 | 1.350 | 110.0 | 375.5 | 507.0 |
| 224 | 0.332 | 1.595 | 115.5 | 348.0 | 555.0 |
| 240 | 0.202 | 1.609 | 67.0 | 331.5 | 533.5 |
| 256 | 0.203 | 1.788 | 66.5 | 328.0 | 586.5 |
| 272 | 0.156 | 1.915 | 60.5 | 387.0 | 741.0 |
| 288 | 0.175 | 2.026 | 67.0 | 382.5 | 775.0 |
| 304 | 0.171 | 1.956 | 67.5 | 395.5 | 773.5 |
| 320 | 0.183 | 1.860 | 76.5 | 417.5 | 776.5 |
| 336 | 0.200 | 1.683 | 96.0 | 480.0 | 808.0 |
| 352 | 0.164 | 1.571 | 87.0 | 530.0 | 832.5 |
| 368 | 0.147 | 1.508 | 71.0 | 482.0 | 727.0 |
| 384 | 0.104 | 1.665 | 50.0 | 478.5 | 796.5 |
| 400 | 0.280 | 1.538 | 130.5 | 466.5 | 717.5 |

5.21

| Blk | RATIOS F1/F2 | RATIOS F3/F2 | COUNTS F1 | COUNTS F2 | COUNTS F3 |
|---|---|---|---|---|---|
| 16 | 0.328 | 2.313 | 104.0 | 317.5 | 734.5 |
| 32 | 0.344 | 2.661 | 102.5 | 298.0 | 793.0 |
| 48 | 0.359 | 1.891 | 123.0 | 343.0 | 648.5 |
| 64 | 0.301 | 1.847 | 102.5 | 340.0 | 628.0 |
| 80 | 0.282 | 1.823 | 97.0 | 344.0 | 627.0 |
| 96 | 0.278 | 2.038 | 97.5 | 351.0 | 715.5 |
| 112 | 0.301 | 2.122 | 95.0 | 315.5 | 669.5 |
| 128 | 0.291 | 1.637 | 98.5 | 339.0 | 555.0 |
| 144 | 0.321 | 2.019 | 111.0 | 345.5 | 697.5 |
| 160 | 0.388 | 1.973 | 120.0 | 309.5 | 610.5 |
| 176 | 0.427 | 2.253 | 128.0 | 300.0 | 676.0 |
| 192 | 0.390 | 1.803 | 125.0 | 320.5 | 578.0 |
| 208 | 0.378 | 2.185 | 116.5 | 308.0 | 673.0 |
| 224 | 0.324 | 1.569 | 82.0 | 253.0 | 397.0 |
| 240 | 0.310 | 2.198 | 100.5 | 324.0 | 712.0 |
| 256 | 0.266 | 2.391 | 78.0 | 293.0 | 700.5 |
| 272 | 0.320 | 2.173 | 115.0 | 359.0 | 780.0 |
| 288 | 0.290 | 2.619 | 83.5 | 287.5 | 753.0 |
| 304 | 0.296 | 2.120 | 102.5 | 346.0 | 733.5 |
| 320 | 0.306 | 3.093 | 75.5 | 246.5 | 762.5 |
| 336 | 0.301 | 2.390 | 102.5 | 341.0 | 815.0 |
| 352 | 0.256 | 1.987 | 98.5 | 385.0 | 765.0 |
| 368 | 0.280 | 1.937 | 109.5 | 391.5 | 758.5 |
| 384 | 0.337 | 2.116 | 105.5 | 313.5 | 663.5 |
| 400 | 0.281 | 2.029 | 102.0 | 363.0 | 736.5 |

heard.21

| | RATIOS | | COUNTS | | |
|---|---|---|---|---|---|
| Blk | F1/F2 | F3/F2 | F1 | F2 | F3 |
| 16 | 0.383 | 1.975 | 147.0 | 383.5 | 757.5 |
| 32 | 0.236 | 1.913 | 95.0 | 403.0 | 771.0 |
| 48 | 0.301 | 1.718 | 124.0 | 411.5 | 707.0 |
| 64 | 0.200 | 1.616 | 87.5 | 436.5 | 705.5 |
| 80 | 0.328 | 1.745 | 123.5 | 377.0 | 658.0 |
| 96 | 0.370 | 2.223 | 125.0 | 338.0 | 751.5 |
| 112 | 0.450 | 2.093 | 160.5 | 356.5 | 746.0 |
| 128 | 0.321 | 2.218 | 113.0 | 351.5 | 779.5 |
| 144 | 0.381 | 2.153 | 130.5 | 342.5 | 737.5 |
| 160 | 0.462 | 1.973 | 137.0 | 296.5 | 585.0 |
| 176 | 0.334 | 2.054 | 102.5 | 306.5 | 629.5 |
| 192 | 0.367 | 2.015 | 121.0 | 330.0 | 665.0 |
| 208 | 0.362 | 2.179 | 113.0 | 312.0 | 680.0 |
| 224 | 0.356 | 1.087 | 114.0 | 320.0 | 348.0 |
| 240 | 0.308 | 1.844 | 109.5 | 356.0 | 656.5 |
| 256 | 0.257 | 1.854 | 99.5 | 387.5 | 718.5 |
| 272 | 0.342 | 1.954 | 114.5 | 335.0 | 654.5 |
| 288 | 0.313 | 2.124 | 113.0 | 361.5 | 768.0 |
| 304 | 0.298 | 2.194 | 107.0 | 359.0 | 787.5 |
| 320 | 0.315 | 1.960 | 123.5 | 392.0 | 768.5 |
| 336 | 0.306 | 2.014 | 110.5 | 361.0 | 727.0 |
| 352 | 0.306 | 1.889 | 114.0 | 372.5 | 703.5 |
| 368 | 0.331 | 2.440 | 101.5 | 307.0 | 749.0 |
| 384 | 0.219 | 1.869 | 95.0 | 434.5 | 812.0 |
| 400 | 0.277 | 2.199 | 100.0 | 361.0 | 794.0 |